NASA TN D-366

TECHNICAL NOTE
D-366

POWER SPECTRAL ANALYSIS OF SOME AIRPLANE RESPONSE QUANTITIES OBTAINED DURING OPERATIONAL TRAINING MISSIONS OF A FIGHTER AIRPLANE

By Harold A. Hamer and John P. Mayer

Langley Research Center
Langley Field, Va.

NATIONAL AERONAUTICS AND SPACE ADMINISTRATION

WASHINGTON

March 1960

NATIONAL AERONAUTICS AND SPACE ADMINISTRATION

TECHNICAL NOTE D-366

POWER SPECTRAL ANALYSIS OF SOME AIRPLANE RESPONSE QUANTITIES OBTAINED DURING OPERATIONAL TRAINING MISSIONS OF A FIGHTER AIRPLANE

By Harold A. Hamer and John P. Mayer

SUMMARY

The frequency content of some airplane response quantities obtained from a number of operational training flights of a fighter airplane is presented. Power spectral densities of normal and transverse load factor and pitching acceleration are shown for several types of missions normally performed by the airplane. The frequency content, which is described by the spectrum, provides information which is useful in control-system design and in the design of recording and computing equipment for analyzing maneuver-load data.

When normalized by dividing by the mean-square value, the results indicate that, except for some differences at the higher frequencies due to the effect of rough air, the frequency content of each of the airplane response quantities was similar during the different types of missions investigated.

The normal-load-factor data were found to exhibit some of the characteristics of a Gaussian random process; therefore, peak distributions for this quantity could be estimated to a good degree of accuracy with the use of spectrum-analysis methods.

INTRODUCTION

In an effort to provide information leading to the establishment of more realistic loads criteria for the design of military airplanes, the National Aeronautics and Space Administration has been conducting a limited flight investigation of the manner in which military airplanes are used in service training operations. The statistical analysis of the control-input and airplane-response data has produced probability distributions of peak values for various load parameters (refs. 1 and 2) and the power spectra of the normal load factor (ref. 3). Such probability distributions can be used in determining the design limits of the

various airplane components as well as in the study of fatigue. A knowledge of the frequency content, which is described by the power spectrum, is useful in the design of automatic or power control systems. The frequency analysis can also be used in work connected with developing instrumentation for recording maneuver-load data and as a guide in developing techniques for reducing and analyzing the flight measurements with automatic computing machinery.

Power spectral densities of normal and transverse load factor and pitching acceleration obtained from a number of operational training flights of a fighter airplane are presented in this report. The spectra are shown for three types of missions as well as for the combined missions. The types of missions are classified as (1) low-altitude bombing system (LABS), (2) dive bombing, and (3) general flying.

The types of missions differ both in the type of maneuvering performed and in the flight conditions (altitude and speed) under which the maneuvering was done. They also differ in the amounts of rough air encountered. During low-altitude-bombing missions, in particular, the large amount of rough air encountered at the low altitudes caused the airplane to experience rather violent lateral and longitudinal oscillations. One purpose of this report is to show the extent to which the power spectra of the response quantities are affected by various types of missions normally performed by the airplane.

In the application of power-spectral-analysis methods, a number of useful theoretical relationships have been established for Gaussian random processes, one of which predicts the frequency of occurrence of peak values. Previous analysis of small samples of data on two different airplanes (ref. 3) indicated that, for the normal load factor in general-flying missions, this relationship provided a reasonably good guide in calculating the number and the probability distribution of peak values. In the present investigation the study of the applicability of this Gaussian process relationship is extended to another airplane and to data samples which are larger and from different types of missions.

SYMBOLS

f frequency, cps

f_0 average number of times per second that mean value of normal load factor is crossed with positive slope,

$$f_0^2 = \frac{\int_0^\infty f^2 \Phi(f)_{\Delta n_v} \, df}{\int_0^\infty \Phi(f)_{\Delta n_v} \, df} \quad \text{(see ref. 4)}$$

f_p average number of positive incremental normal-load-factor peaks per second, $f_p^2 = \dfrac{\int_0^\infty f^4 \Phi(f)_{\Delta n_v}\, df}{\int_0^\infty f^2 \Phi(f)_{\Delta n_v}\, df}$ (see ref. 4)

$f(t), y(t)$ time history of a quantity

$F(2\pi if)$ Fourier transform of $f(t)$, $\int_0^\infty f(t) e^{-2\pi ift} dt$

g acceleration due to gravity, ft/sec^2

K constant used in filter equation

m total number of observations

M Mach number

n_t transverse load factor

n_v normal load factor

Δn_v incremental normal load factor, $n_v - 1$

N number of positive incremental normal-load-factor peaks exceeding a given value

$P(\Delta n_v)$ probability that a given value of Δn_v will be exceeded for a truncated normal distribution

P_p probability that a peak value of Δn_v will exceed a given value for a Gaussian random process

$\dot{q}$ pitching acceleration, $radians/sec^2$

t time, sec

Δt time reading interval, sec

T time interval of $f(t)$ or $y(t)$, sec

T_F flight time analyzed for normal load factor in a given type of mission, sec

T_M maneuvering flight time (defined as time for which $\Delta n_V > 0.25g$), sec

y quantity such as n_V, n_t, or $\dot{q}$

$\bar{y}, \overline{y(t)}$ mean value of y

$y^*(t)$ filtered value of y at time t, $Ky(t - \Delta t) - 2y(t) + Ky(t + \Delta t)$

σ root-mean-square value of y, $\sigma^2 = \dfrac{\sum (y - \bar{y})^2}{m} = \displaystyle\int_0^\infty \Phi(f)_y \, df$

$\Phi(f)_y$ power spectral density of y,

$$\lim_{T \to \infty} \frac{1}{T} \left| \int_{-T}^{T} \left[y(t) - \overline{y(t)} \right] e^{-2\pi i f t} dt \right|^2 \quad \text{(see ref. 5)}$$

$\Phi(f)_{y^*}$ power spectral density of y^*

AIRPLANE

A photograph of the test airplane is presented in figure 1. The test airplane is a single-place jet-propelled fighter-bomber airplane having a swept wing and swept tail surfaces. The airplane is equipped to carry a wide assortment of weapons and external fuel tanks.

All control surfaces are actuated by an irreversible hydraulic-powered boost system. Control feel is simulated by artificial-feel devices which vary the feel in proportion to stick or rudder pedal deflection. A one-piece stabilator is used for longitudinal control. A control-stick damper is incorporated to prevent overcontrol by restricting the speed at which the control stick can be moved in the longitudinal direction. A mechanical ratio shifter is incorporated in the system so that with the landing gear retracted the control-stick travel per degree of stabilator movement is increased to reduce control sensitivity. Included in the lateral-control system are spoilers which are located on the upper surface of both wings immediately forward of the flaps. The spoilers are actuated by the control-stick lateral deflection. The spoilers operate when the landing gear is in the retracted

position and move in the up-direction only. As the aileron moves up from 0° to about 11°, the corresponding spoiler moves up proportionally from 0° to about 45° and remains at 45° for the remainder of aileron travel. A hydraulically operated speed brake is installed on each side at the rear of the fuselage.

Neither the external appearance (except for the installation of a nose boom) nor the weight and balance of the airplane was altered by the addition of the instrumentation. A three-view drawing of the test airplane is presented in figure 2. Tables showing dimensions and physical and mass characteristics are given in reference 2.

INSTRUMENTATION

The data were measured by the use of standard NASA photographic recording techniques. An airspeed-pressure switch was employed to operate the recording instruments automatically at speeds above 100 knots.

Normal and transverse load factors with respect to the airplane longitudinal reference axis (see fig. 2) were measured by an NASA magnetically damped, three-component recording accelerometer. The accelerometer was mounted near the average "in-flight" center of gravity in such a way that the effects of airplane angular velocities and angular accelerations on the load-factor measuring elements could be considered negligible for this analysis. Pitching-acceleration measurements were obtained by an angular acceleration recorder containing a gyroscopic sensing element. The recording-instrument elements were damped to about 0.65 of critical damping and their natural frequencies were selected to minimize the magnitude of extraneous airplane vibrations.

A standard two-cell pressure recorder connected to the airplane service system was used to measure static and impact pressures for determining the pressure altitude, indicated airspeed, and Mach number. The service system included a total-pressure tube and flush static-pressure orifices. No corrections were made to the measurements for position error associated with the location of the static-pressure orifices. More detail on the instrumentation and accuracy of the measurements is given in reference 2.

TESTS

The flights were made by 23 service pilots undergoing regular squadron operational training at Langley Air Force Base, Va. Approximately 45 hours of flight time was recorded during 53 operational flights made

from November 1955 to April 1956. Data were recorded continuously throughout a flight but were recorded only during those flights in which the mission was scheduled to include a large number of maneuvers; that is, no cross-country or instrument flights were recorded. No attempt was made to specify the type or severity of maneuvers. Some of the flights during the general-flying missions were made with the clean airplane configuration and some with various arrangements of external fuel tanks and bombs. All flights during the low-altitude-bombing and dive-bombing missions were made with these external stores.

The results are representative of the various tactical maneuvers that are within the capabilities of the airplane. Although not requested, most of the maneuvers were performed in relatively smooth air except where the usual turbulence near the ground was encountered. Data were recorded at altitudes from ground level to about 42,000 feet, at indicated airspeeds varying from the stalling airspeed to about the maximum service-limit airspeed (610 knots), and at Mach numbers up to about 1.1. A summary of the flight conditions for the different types of missions is presented in figures 3 to 5 in the form of the percentages of time in various airspeed, Mach number, and altitude ranges. The data given in these figures are based on the flight time analyzed T_F rather than on total flight time recorded.

CLASSIFICATION OF MISSIONS

The flights have been classified under three types of missions: (1) low-altitude-bombing system (LABS), (2) dive bombing, and (3) general flying. Six comparatively straight and level flights (4.4 flight hours) were made which contained few maneuvers; data from these flights are not included in the final results except where indicated in the section entitled "Results and Discussion."

Low-Altitude-Bombing System

The data pertaining to low-altitude-bombing missions consisted of 13 flights (12.6 flight hours) which were devoted to practicing low-altitude-bombing maneuvers. The low-altitude-bombing data represent a total of 98 maneuvers inasmuch as each pilot made an average of 7 or 8 of these maneuvers in each flight. During these tests some of the maneuvers were simulated (no bombs dropped) and in some, a small practice bomb or a 1,700-pound practice bomb was dropped. The low-altitude-bombing maneuver consists of a straight-and-level pass at high speed (approximately 500 knots) near the ground, and an abrupt pullup to a prescribed normal load factor of 4, the bomb automatically releasing

at a predetermined airplane attitude angle. After the bomb is released, the half-loop is carried to completion and a 180° roll is made at the top, the entire maneuver actually being an Immelmann turn.

Two types of deliveries were performed in the low-altitude-bombing missions: over-the-shoulder delivery and initial-point delivery. For the over-the-shoulder delivery the pullup is made directly over the target and the bomb is released at an airplane attitude angle which is greater than 90°. In the initial-point delivery the pullup is made when a predetermined time has elapsed after passing over a point which has been selected in front of the target. In comparison with the over-the-shoulder delivery, the bomb is released at a smaller attitude angle while the airplane is still at a distance in front of the target.

L
7
7
8

Dive Bombing

The dive-bombing data were obtained from 6 flights (6.1 flight hours) which were flown solely for the purpose of practicing dive-bombing techniques. Each flight consisted of a number of dive-bomb runs, with a total of 50 for the 6 flights. Some of the maneuvers were simulated, whereas in others small practice bombs were dropped.

One of the 6 flights consisted of 10 of the more common type of runs in which the dive is made from an altitude of about 8,000 feet with the bomb release and pullout started at about 3,000 feet. In the remaining 5 flights all the dive-bombing runs were made from high altitude. Here the dives began at altitudes as high as 20,000 feet and the pullouts were started anywhere from 16,000 to 12,000 feet.

General Flying

The missions classified under general flying are a collection of many types of maneuvers and correspond to all flights which were not made for the sole purpose of performing low-altitude-bombing or dive-bombing maneuvers. Most of these flights were familiarization flights, in which the pilots performed all types of acrobatic maneuvers and in some cases several simulated low-altitude-bombing and dive-bombing maneuvers. Other flights in this category of general flying included simulated strafing, formation flying, and "rat racing." The general-flying data represent 28 flights with a total of 21.9 hours of flight time.

METHODS OF ANALYSIS

The analysis used to determine the power spectra and peak probability distributions parallels that of reference 3. The frequency content of a time history of a quantity $f(t)$ is ordinarily given as the amplitude of the Fourier transform:

$$F(2\pi if) = \int_0^\infty f(t)e^{-2\pi ift}dt \tag{1}$$

The power spectrum given by the equation

$$\Phi(f) = \lim_{T\to\infty} \frac{1}{T}\left|\int_{-T}^{T} f(t)e^{-2\pi ift}dt\right|^2 \tag{2}$$

is a convenient way of presenting the frequency content of a long time history of a quantity. Essentially, the power spectral densities may be considered proportional to the amplitude squared of the frequency content ordinarily obtained from the Fourier transform. Thus, the power spectrum can be regarded as a frequency analysis of the mean-square value of the random time function $f(t)$.

Record Evaluation for Power Spectra

The numerical methods described in reference 5 were used in determining the power spectral densities. Records for the various quantities were read at given time intervals, and 40 estimates of the power at frequencies up to the folding frequency $1/2\Delta t$ were obtained by using digital computing methods. Record readings were made during maneuvering portions of the flights and include takeoff and landing data for the times when the airplane was airborne. An explanation as to what constituted the maneuvering portions of the time histories for each quantity is given subsequently. These portions are different for each quantity and were determined by deleting certain sections of the time histories. The effect of omitting sections of the time-history data on the shape of the spectrum has been found to be negligible in this type of analysis (ref. 3); only the level of the spectrum is changed.

The power spectra presented are the spectra of the time history with the mean subtracted $\Phi(f)_{(y-\bar{y})}$. Power spectral densities for each quantity were first obtained on a per-flight basis. In cases where spectral

densities are presented according to a specific type of mission, in which the data for more than one flight are included, the power spectrum presented is an average of the spectra that were calculated for each of the flights pertaining to the mission. The average was weighted according to the time analyzed in each of the flights.

The normal-load-factor time histories were read at a time interval of 0.5 second to provide estimates of power up to a frequency of 1 cycle per second. From these readings, power spectral densities were calculated by using time intervals of 0.5, 2, and 10 seconds to provide adequate detail over the frequency range. In addition, the normal-load-factor spectra were computed for several flights by using 0.2-second reading intervals to provide additional information at frequencies up to 2.5 cycles per second.

All the records of transverse load factor were evaluated at time intervals of 0.5 second. For several flights, however, the spectra for transverse load factor were obtained out to a frequency of 2.5 cycles per second through the use of 0.2-second readings.

Spectra for pitching acceleration were obtained at frequencies up to 2 cycles per second by reading the time histories at intervals of 0.25 second.

In order to improve the accuracy of the computed spectra, the spectrum was first obtained of an altered (filtered) time history of the quantity given by the equation

$$y^*(t) = Ky(t - \Delta t) - 2y(t) + Ky(t + \Delta t) \qquad (K < 1) \qquad (3)$$

This equation is essentially a high-pass numerical filter which, for $K < 1$, retains some information at zero frequency. This particular expression was used because it was found to make the spectra relatively constant over the frequency range when the appropriate value of K was used. The values of K used varied from 0.97 to 0.70 for the spectra presented in this report. The spectrum of y^* was then converted to the spectrum of y by the equation

$$\Phi(f)_y = \frac{\Phi(f)_{y^*}}{\left[2K \cos(2\pi f \Delta t) - 2\right]^2} \qquad (4)$$

The data at 10-second intervals were not filtered by using equation (3) since the spectrum for the frequency range covered was relatively level.

Flight Conditions and Flight Time Analyzed

As previously indicated the flight conditions for each type of mission are summarized in figures 3 to 5 as the percentages of time at various airspeeds, Mach numbers, and altitudes. These distributions are based on the flight time T_F in each type of mission rather than total flight time recorded in each type of mission and are representative of the flight conditions under which the spectra were obtained. The time T_F for total missions was approximately 65 percent of the total flight time recorded in the investigation. (Distributions of airspeed, Mach number, and altitude were calculated for the total flight time recorded and were found to be about the same as those shown for the flight time T_F.) The flight time T_F is the time for which the normal-load-factor data were analyzed. This time is defined as that time which included all portions of the flights where any noticeable maneuvering was taking place and was based on movement of the film trace for normal load factor. Thus, all relatively long portions of straight and level flight were eliminated. For instance, for the low-altitude-bombing and dive-bombing missions, the data recorded during the time to and from the practice range were not analyzed since these data represented essentially nonmaneuvering flight. Also, in the general-flying missions there would be long periods during which little or no maneuvering was occurring; therefore, these times were not analyzed. No attempt was made to eliminate data during the shorter periods of near-level flight which occurred between the various maneuvers in the general-flying flights or between the practice runs in the low-altitude-bombing and dive-bombing flights.

Spectra for transverse load factor and pitching acceleration were obtained from data taken from the portions of flight which included the time T_F. These spectra do not include data for all the time T_F, however, as only those sections of the transverse-load-factor and pitching-acceleration time histories were read which showed any noticeable fluctuations. Furthermore, the pitching-acceleration data were not analyzed for all flights. The pitching-acceleration spectra shown for the low-altitude-bombing and dive-bombing missions correspond to three flights each and the spectrum for general flying missions is for 22 out of the total of 28 flights pertaining to this type of mission. The flights selected for the analysis of pitching acceleration are considered to give spectra which are representative of the different types of missions.

Normal-Load-Factor Counts

In order to examine the statistical properties of the loads, several methods were used to take counts of normal load factor from the time histories. One of the methods employed a threshold-counting process which

minimized the level-flight portions of the time histories occurring during and between maneuvers. The probability distributions resulting from this type of count are compared with the probability distributions that would be obtained for a Gaussian random process. In the other method, peak values were counted from which major peak and total peak distributions were determined. These peak distributions are compared with the peak distributions calculated from the power spectra. A description of each of the counting methods follows.

Threshold count.- The method used is identical to that illustrated in reference 3. Only load factors of 1 or greater were counted. In this method counts were made at a given threshold every time the record crossed the given threshold and exceeded one-half of the increment to the next threshold. Threshold values of 0.5g were used. For example, counts were made at a normal load factor of 2 if the load-factor record crossed 2g while increasing and then increased above 2.25g or if the record crossed 2g while decreasing and decreased below a value of 1.75g. By using this method all small fluctuations in the normal load factor less than ±0.25g are eliminated.

Major peak count.- The method employed to determine the major peaks is the same as one of the methods illustrated in reference 3. Only peaks above a load factor of 1 were considered. The peaks counted by this method reflect the major positive excursions of normal load factor from the level-flight value and ignore the smaller fluctuations. In this method a peak was counted if the load factor decreased both before and after the peak by an amount more than one-quarter of the value of the peak increment, the peak increment being measured from a normal-load-factor value of 1. In addition to this, for normal load factors less than 2 the load factor had to decrease more than 0.25g before and after the peak in order to be counted. By using this method of determining peaks, all small fluctuations in the load factor due to airplane vibrations and other small disturbances are eliminated.

Total peak count.- The total peak count includes all peaks above 1.25g obtainable from the time histories. The reading accuracy for normal load factor was 0.01g; therefore, these peaks represent all fluctuations greater than 0.01g.

RESULTS AND DISCUSSION

The power spectra of the airplane response quantities define the frequency range which can be considered as being important for these quantities in the analysis of maneuver-load data. For example, if the frequency content of normal-load-factor data during maneuvering were negligible above frequencies of 2 cycles per second, it would be necessary to use recording and computing equipment capable of measuring and

analyzing these data only in the frequency range up to 2 cycles per second. Power spectra of the airplane response would also be useful in control-system design. For instance, the control system of an airplane would have to be designed with good frequency response only for the important frequency range of the response quantities.

Inasmuch as the frequency characteristics of the control system of the airplane could influence the frequency content obtained for the airplane response, these characteristics were examined. It was found that the frequency response of the control system was flat over the range of frequencies analyzed in this report ($0 < f < 2.5$ cycles per second) and that the control system was capable of responding considerably beyond these frequencies; therefore, the frequency characteristics of the control system would have little effect on the results obtained.

L 7 7 8

Normal Load Factor

Normal-load-factor data are presented in figures 6 to 13. Power spectral densities, which have been normalized by dividing by the mean-square value σ^2 corresponding to the particular data sample, are shown in figures 6 to 9 and probability data are shown in figures 11 to 13. The probability data are given in terms of incremental normal load factor Δn_y. Results presented for total missions in figures 6, 7, 11, 12, and 13 include data from the six comparatively straight and level flights previously mentioned in the section entitled "Classification of Missions."

Power spectral densities.- In figure 6 spectra are shown for each of the three types of missions as well as for total missions. The spectra are composed of spectral densities calculated from record time-interval readings of 0.5, 2, and 10 seconds. The spectra given in figure 6 are for the maneuvering portions of the flights - that is, long periods of straight and level flight have been deleted - and it is of interest to note that the root-mean-square value σ is about the same during any type of mission. Because the spectrum for the total missions includes additional data from six comparatively straight and level flights where only a few mild maneuvers were performed, the value of σ for the total missions is slightly lower than that for any of the three types of missions.

Because power spectra are statistical in nature, some knowledge of the statistical reliability of spectra such as given in figure 6 is important. Each value of power given in the figure is the average of the estimates made at a given frequency for each of the flights in a particular type of mission. For example, for a frequency of 0.1 cycle per second the value of 0.70 per cycle per second given in the general-flying spectrum is the average of 28 values obtained from 28 flights. For each of

these flights, the power-spectral-density estimates were made from about 4,000 data points. For spectral-density calculations based on 40 estimates, there would thus be about 200 degrees of freedom available in each estimate of the power-spectral-density value (see ref. 6). It would be expected then that, for stationary random processes, estimates with 200 degrees of freedom would depart from the long run average by ±14 percent at the 80-percent confidence level, or for the present example, in which the long run average is 0.70, 10 percent of the time the estimate would be expected to fall below 0.602 and 10 percent of the time above 0.798. For the 28 flights the estimates of power at a frequency of 0.1 cycle per second were distributed approximately normally about the mean 0.70 with a standard deviation of 0.226; thus, 10 percent of the estimates were below 0.41 and 10 percent exceeded 0.99. A similar comparison was found in general flying at frequencies of 0.4 and 0.7 cycle per second as well as in low-altitude-bombing and dive-bombing missions at 0.1, 0.4, and 0.7 cycle per second. From this comparison it is seen that the range in variability for the spectral density in the average spectrum is three times greater than that which is expected for stationary random processes.

In figure 7, where the spectra for the different types of missions are compared, the power spectral densities appear to be very similar over much of the frequency range in that they decrease approximately as $f^{-2.5}$. The noticeable leveling off at high frequency in the spectra for low-altitude-bombing and total missions is caused by the effect of rough air encountered at high speeds during low-altitude-bombing maneuvers. In these maneuvers turbulence encountered during the high-speed runs at altitudes near the ground produced load-factor oscillations near the longitudinal short-period oscillation frequency of the airplane. In addition, the normal-load-factor oscillations were magnified by the inadvertent lateral oscillations of the airplane associated with the high speeds and the turbulent air. During this investigation the low-altitude-bombing and dive-bombing practice runs were, for the most part, made in a periodic fashion and this effect is evident in the spectra. The predominant peak in the low-altitude-bombing and dive-bombing spectra at about 0.01 cycle per second corresponds to the average number of bombing runs per second in the dive-bombing flights and the average number of maneuvers per second during the low-altitude-bombing flights, which was roughly 36 per hour. (Each low-altitude-bombing run usually consisted of two maneuvers, the turn into the high-speed run and the pullup for the bomb release.)

In order to show additional data on the effect of rough air, several flights were read at 0.2-second intervals to extend the frequency range for the spectra up to 2.5 cycles per second. These results are shown in figures 8 and 9. The spectrum for one low-altitude-bombing flight is shown in figure 8 and is composed of spectral densities calculated from record time-interval readings of 0.2, 0.5, and 2 seconds. The peak in the spectrum at approximately 1 cycle per second is caused by the rough air; however, there is very little power (portion of the root mean square) in this frequency range of about 0.5 to 2.5 cycles per second. The peak

near 0.01 cycle per second caused by the frequency of maneuvers (see low-altitude-bombing spectrum in fig. 6) does not appear in this figure because the spectrum for this flight was not calculated for 10-second intervals to give detail at these low frequencies.

The spectrum for a relatively straight and level flight through a large amount of turbulence is shown in figure 9. This flight was essentially a nonmaneuvering flight at moderate speeds (M = 0.53 to 0.73) and was made at altitudes from 5,000 feet to near sea level. The only maneuvers performed were a few gentle turns. It can be seen that the power spectral densities are fairly constant over the frequency range up to the vicinity of the longitudinal short-period oscillation frequency and then decrease rapidly at higher frequencies. The spectral densities shown were calculated from record readings made at 0.2-second intervals.

The data given in figures 8 and 9 are compared in figure 10. The frequency content is more graphically illustrated if $f\Phi(f)$ is plotted against $\log_e f$. For example, the mean-square value

$$\sigma^2 = \int_0^\infty \Phi(f)df \tag{5}$$

can be expressed as

$$\sigma^2 = \int_0^\infty f\Phi(f)d \log_e f \tag{6}$$

In figure 10, where $f\Phi(f)_{n_v}$ is plotted against $\log_e f$, the portion of the root mean square contributed by a given frequency band is directly proportional to the area under the curve in that band. The low-altitude-bombing-system curve is representative of normal load factors experienced on fighter airplanes during maneuvering in rough air. For this curve it can be seen that the area is concentrated at a frequency of about 0.02 cycle per second. From the curve for the relatively straight and level flight in rough air it can be seen that there is only a small amount of power at frequencies below 0.1 cycle per second. By comparing the peaks in the two curves occurring at about 1 cycle per second, it is apparent that the peak at this frequency in the low-altitude-bombing spectrum is an effect of turbulence rather than of maneuvering. It is also apparent that this effect of rough air during maneuvering contributes little to the root-mean-square normal load factor.

Probability distributions.- It was found in reference 3 that for general-flying type of maneuvers, the threshold counts of positive incremental normal load factor could be described by a truncated normal distribution. If the normal-load-factor data are assumed to be truncated at $\Delta n_v = 0$ and the mean of the parent distribution is assumed to be at $\Delta n_v = 0$,

$$P(\Delta n_v) = \frac{1}{0.5\sqrt{2\pi}} \int_{\Delta n_v/\sigma}^{\infty} e^{-\frac{1}{2}\left(\frac{\Delta n_v}{\sigma}\right)^2} d\left(\frac{n_v}{\sigma}\right) \qquad (\Delta n_v \geqq 0) \qquad (7)$$

which defines the probability that a given value of Δn_v will be exceeded for the truncated normal distribution.

Normal probability graph paper can be used as a simple qualitative test for a normal distribution. The scales on this paper are adjusted so that the probabilities for given values of a quantity will plot as a straight line if the frequency distribution is normal. This type of plot is shown in figure 11 for the various types of missions using the probabilities obtained from the threshold counts. Since the normal-load-factor data are truncated, the ordinate scale is given in terms of the quantity $0.5 \times P(\Delta n_v)$. (See eq. (7).) The points shown in the plots are plotted at 0.25g less than the threshold values (that is, 1 plotted at 0.75, 1.5 plotted at 1.25, and so forth) since the thresholds were based on bands $\pm$0.25g about the threshold values. In each plot the number of counts for the zero threshold (the number of counts for the band -0.25g to 0.25g) was adjusted by multiplying the zero-threshold crossings actually counted by a factor of 2. Straight lines representing normal truncated distributions were faired through the data points. For a normally distributed set of data, 34.1 percent of the measurements fall into the interval from the mean to one standard deviation; therefore, the root mean square σ in each plot was obtained directly from the intersection of the straight line with the 0.159 value for $0.5 \times P(\Delta n_v)$. The general-flying data can be considered as being reasonably close to a normal distribution. As would be expected, truncated normal distributions are not so good a fit to the low-altitude-bombing, dive-bombing, and total data because of the nature of these missions.

Although the normal-load-factor data pertaining to the various types of missions cannot be considered a Gaussian random process, results in figure 11 indicate that the positive incremental normal load factors can be considered as a truncated normal distribution. Hence, the expression for the peak probability distribution for a Gaussian random process (ref. 4) was used as a guide to calculate peak distributions from information obtained from the power spectra. Equations derived from this expression and given in reference 3 were used to estimate the total peak

and major peak distributions. The total number of positive peaks exceeding a given value is

$$N = f_p T_M P_p \tag{8}$$

where the quantity P_p is the probability that a peak will exceed a given value for data which are Gaussian in character. The equation for determining P_p from properties of the power spectrum is given in reference 3. The equation used to estimate the number of major peaks exceeding a given value is

$$N \approx f_0 T_M e^{-\frac{1}{2}\left(\frac{\Delta n_v}{\sigma}\right)^2} \tag{9}$$

It can be noted that maneuvering flight time T_M is used in equations (8) and (9). As previously indicated, only those portions of the normal-load-factor time histories which did not include long periods of straight and level flight were analyzed. Even in these portions, however, much time was spent at normal load factors for near level flight during many types of maneuvers and also between the maneuvers. In order to determine the value of T_M to be used in the calculations, the percentage of time spent above a given incremental normal load factor was determined for the flight time analyzed T_F. These percentages are shown in figure 12 for each type of mission and for total missions. Since in the threshold counts and in the peak counts the minimum normal-load-factor variation was 0.25g, it was assumed that the maneuvering flight time T_M was the portion of time spent above an incremental normal load factor of 0.25g. It can be seen in the figure that about 40 percent of the flight time analyzed can be considered maneuvering flight time for general-flying, dive-bombing, and total missions and about 47 percent for low-altitude bombing. The value of the root-mean-square incremental normal load factor σ used in the calculations must correspond to the load-factor data associated with T_M. The value of σ was, therefore, established from the threshold counts, as this type of count minimized the data for near level flight.

The peak distributions as given by equations (8) and (9) are shown in figure 13 for the various types of missions. The value of the root-mean-square incremental normal load factor σ used was that obtained from the threshold analysis shown in figure 11. The values for f_p and f_0 were obtained from the integration of the spectra and are given in figure 13. The peak distributions obtained from peak counts made on the

time histories are also shown in the figure by the circular and square symbols. The major peaks and total peaks were counted by the methods given in a previous section.

It may be seen in figure 13 that, for general flying, both the total peak count and the major peak count are estimated to a good degree of accuracy by equations (8) and (9), respectively. The agreement between the calculated and observed distributions for the low-altitude-bombing, dive-bombing, and total missions is not as good as that for general flying in the low range of Δn_V values. For the larger Δn_V values, however, there appears to be good agreement.

Total peak distributions are of interest but major peak distributions would probably be of the most value, for example, in fatigue analysis. In each plot given in figure 13 it can be seen for the region where calculated and observed results differ that, for the most part, the calculations overestimate the number of peaks at a given Δn_V level.

Transverse Load Factor

Power spectra of transverse load factor are presented in figures 14 to 18. The spectral densities have been normalized by dividing by the mean square σ^2 of the corresponding data sample. Inspection of peak probability distributions given in reference 2 for this airplane indicated that the transverse-load-factor data in low-altitude-bombing and general-flying missions could not be characterized as a Gaussian random process; therefore, the peak distributions were not determined from the power spectrum. One reason for the low-altitude-bombing data not being Gaussian in character was due to the influence of large, constant-amplitude lateral oscillations that were produced during turbulence in many of the low-altitude-bombing maneuvers. Similarly, during the general-flying missions several pilots performed fishtail maneuvers which produced a number of large-amplitude oscillations.

Spectra are shown in figure 14 for each type of mission and for total missions. As previously indicated, the spectra are for those portions of flight where noticeable fluctuations occurred in the transverse-load-factor time history. From the figure it can be seen that the value for σ was small, varying from about 0.030 for general flying and dive bombing to about 0.042 for low-altitude bombing.

In figure 15 it appears that the frequency content for transverse load factor, as defined by the spectrum, is about the same for the various types of missions. The peak in each spectrum at the higher frequencies is near the lateral short-period oscillation frequency of the airplane for high speeds. Although more rough air was present in the

low-altitude-bombing missions, some turbulence was encountered during the other missions. The turbulence accounted for many of the transverse motions of the airplane and caused the airplane to oscillate at the lateral short-period oscillation frequency. The low-altitude-bombing-system spectrum has the most pronounced peak because of the larger amount of turbulence encountered.

In figure 16 an example is shown where $f\Phi(f)_{nt}/\sigma^2$ is plotted against $\log_e f$ for two types of missions. The curves in the figure are for the two spectra showing the largest differences in the spectral densities in figure 15. In figure 16 the portion of the root mean square contributed by a given frequency band is directly proportional to the area under the curve in that band. (See eq. (6).) From the figure it can be seen that the main differences in the spectra occur at the high frequencies. A large proportion of the total area is concentrated at the higher frequencies for low-altitude-bombing missions. It may be shown that about 75 percent of the root-mean-square value is contained at frequencies above 0.5 cycle per second for this type of mission.

Additional examples of spectra pertaining to low-altitude-bombing flights are shown in figure 17. The spectrum in the top plot is shown as a matter of interest and was obtained from two low-altitude-bombing flights made in extremely rough air. In contrast to the spectrum for all the low-altitude-bombing flights (fig. 14) the peak at the high frequency is sharper and the value of σ is larger. In order to define the high-frequency peak more adequately, the transverse-load-factor time history for one low-altitude-bombing flight was read at 0.2-second intervals and thus the spectrum was extended out to a frequency of 2.5 cycles per second. This spectrum is shown in the bottom plot in figure 17 and is composed of spectral densities calculated from record time-interval readings of 0.2 and 0.5 second. In this plot the spectral densities at frequencies above about 1 cycle per second are seen to decrease as the frequency increases.

In figure 18 examples of power spectra of transverse load factor are shown for rough-air and smooth-air flight. The spectrum in the top plot was obtained from a nonmaneuvering portion of a flight (M = 0.6 to 0.7) which was at low altitude (approximately 1,000 feet) in rough air. It can be seen from the spectrum that practically all the root-mean-square value was contained at the higher frequencies associated with the inadvertent lateral oscillations of the airplane.

The spectrum shown in figure 18 for the smooth-air flight was obtained from a general-flying mission in which no rough air was encountered. All transverse load factors obtained in this flight were produced by maneuvering. The spectrum is shown for frequencies out to 2.5 cycles per second and was obtained with the use of 0.2- and 0.5-second record

readings. For this spectrum it is seen that the spectral densities are essentially constant at frequencies up to about 0.6 cycle per second and then drop rapidly in value at higher frequencies. This is in contrast to normal-load-factor spectral densities (fig. 7) which generally decrease over the frequency range. The relatively constant values of transverse-load-factor spectral density can probably be attributed to the lateral short-period oscillations of the airplane. These oscillations are excited during the normal process of maneuvering the airplane and occur at frequencies from about 0.3 cycle per second at low speeds to about 0.7 cycle per second at the higher speeds. The fact that a large portion of the root-mean-square transverse load factor during maneuvering is due to these oscillations would cause the spectrum to be relatively flat over the frequency range indicated in the plot.

L
7
7
8

Pitching Acceleration

The power spectral densities for pitching acceleration are shown in figures 19 and 20 and have been normalized by dividing by σ^2. Peak distributions were not determined from the power spectrum. Inspection of peak probability distributions given in reference 2 indicated that pitching-acceleration data on this airplane were not characteristic of a Gaussian random process during general flying, probably because of the effect of the large values of pitching acceleration occurring in pitch-ups. The pitching-acceleration data during low-altitude bombing and dive bombing, however, did appear to be Gaussian in character.

Records of pitching acceleration were read at 0.25-second intervals so that spectra could be calculated for frequencies out to 2 cycles per second. As in the case of transverse load factor, the spectra are for those portions of flight where noticeable fluctuations occurred in the pitching-acceleration time history. It is of interest to note that the value of σ for the low-altitude-bombing missions was about twice that for general-flying or dive-bombing missions. (See fig. 19.)

The spectral densities for each type of mission are shown on a single plot in figure 20 for purposes of comparison. Although there are some differences in the spectral densities, the shapes of the spectra are similar so that the frequency content of pitching acceleration could be considered to be about the same for any of the types of missions. When the low-altitude-bombing spectrum is compared with those for general flying and dive bombing, it is seen that the low-altitude-bombing spectrum has a sharper high-frequency peak and that this peak occurs at a higher frequency (about 1.4 cycles per second). The characteristics of the low-altitude-bombing spectrum are reflected in the spectrum for total missions. The peak in the low-altitude-bombing spectrum is associated with the large amount of turbulence and high airspeeds for this

type of mission. The frequency at which the peak occurs in the general-flying and dive-bombing spectra (about 0.9 cycle per second) corresponds to the longitudinal short-period oscillation frequency of the airplane for high-speed flight.

The spectra shown for pitching acceleration could not be corrected for folding because the spectral densities at frequencies above 2 cycles per second were not determined. It is believed, however, that, when these corrections are included, the spectral densities will drop rapidly as the frequency increases above about 2 cycles per second. This rapid decrease in spectral-density value is apparent in the spectrum for dive bombing.

L
7
7
8

CONCLUDING REMARKS

The frequency content of some airplane response quantities obtained from a number of operational training flights of a fighter airplane has been presented. Power spectral densities of normal and transverse load factor and pitching acceleration are shown for several types of missions normally performed by the airplane. The frequency content, which is described by the spectrum, provides information which is useful in control-system design and in the design of recording and computing equipment for analyzing maneuver-load data.

When normalized by dividing by the mean-square value, the results indicate that, except for some differences at the higher frequencies due to the effect of rough air, the frequency content of each of the airplane response quantities was similar during the different types of missions investigated.

The normal-load-factor data for the different types of missions exhibited some of the characteristics of a Gaussian random process; therefore, power-spectral methods were used in analyzing the maneuver-load data. Normal-load-factor peak distributions were estimated to a reasonable degree of accuracy from this spectrum analysis. Peak distributions for transverse load factor and pitching acceleration were not determined from the power spectrum because in most types of missions these quantities did not appear to have the characteristics of a Gaussian random process.

Langley Research Center,
National Aeronautics and Space Administration,
Langley Field, Va., January 26, 1960.

REFERENCES

1. Mayer, John P., Hamer, Harold A., and Huss, Carl R.: A Study of the Use of Controls and the Resulting Airplane Response During Service Training Operations of Four Jet Fighter Airplanes. NACA RM L53L28, 1954.

2. Hamer, Harold A., and Mayer, John P.: Statistical Data on Control Motions and Airplane Response of a Republic F-84F Airplane During Operational Training Missions. NASA TN D-386, 1960.

3. Mayer, John P., and Hamer, Harold A.: Applications of Power Spectral Analysis Methods to Maneuver Loads Obtained on Jet Fighter Airplanes During Service Operations. NACA RM L56J15, 1957.

4. Huston, Wilber B., and Skopinski, T. H.: Probability and Frequency Characteristics of Some Flight Buffet Loads. NACA TN 3733, 1956.

5. Press, Harry, and Tukey, J. W.: Power Spectral Methods of Analysis and Their Application to Problems in Airplane Dynamics. Vol. IV of AGARD Flight Test Manual, Pt. IVC, Enoch J. Durbin, ed., North Atlantic Treaty Organization (Paris), pp. IVC:1-IVC:41.

6. Blackman, R. B., and Tukey, J. W.: The Measurement of Power Spectra. Dover Pub., Inc., 1959.

Figure 1.- Test airplane. L-91212

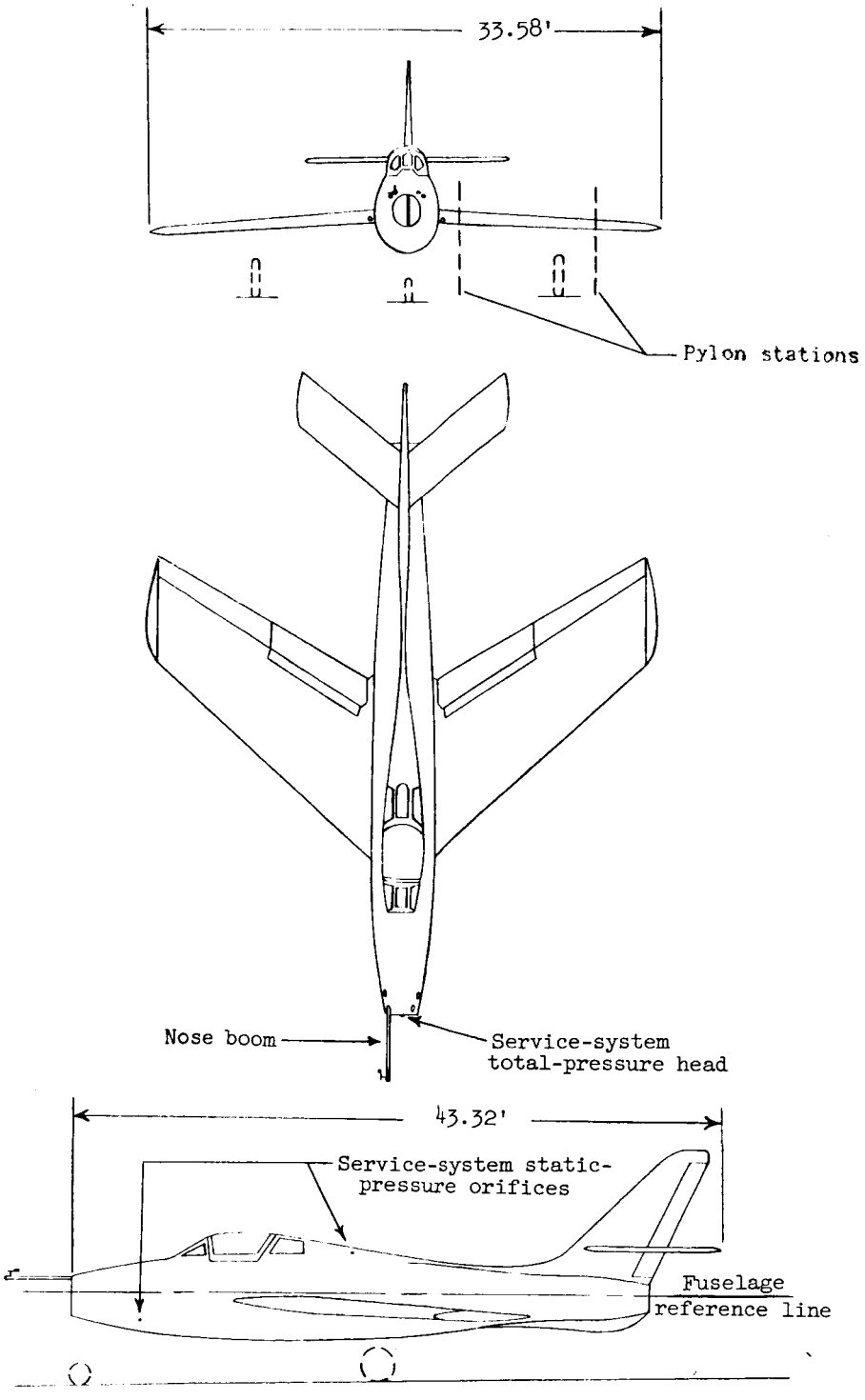

Figure 2.- Three-view drawing of test airplane.

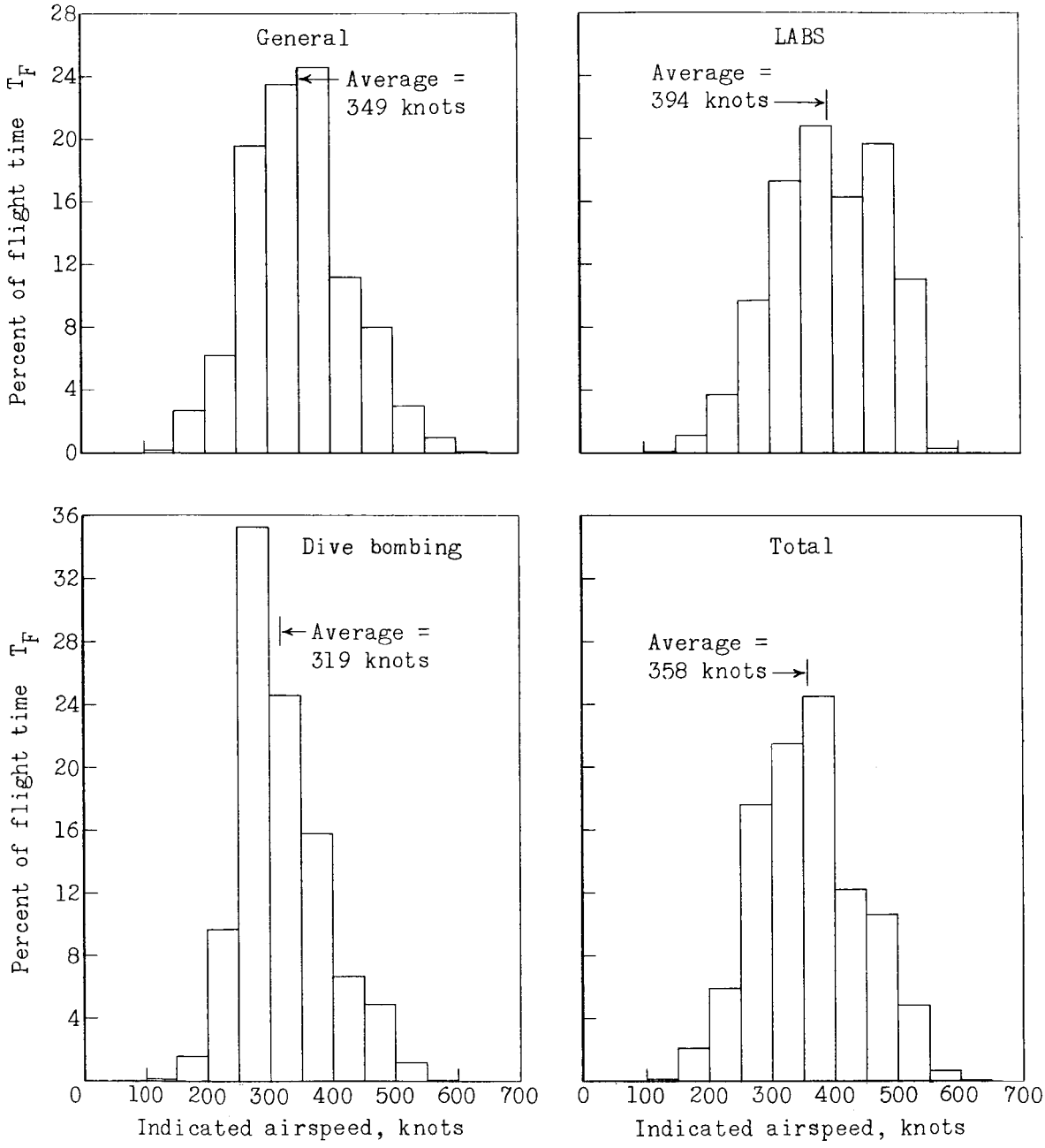

Figure 3.- Distribution of indicated airspeed for various types of missions.

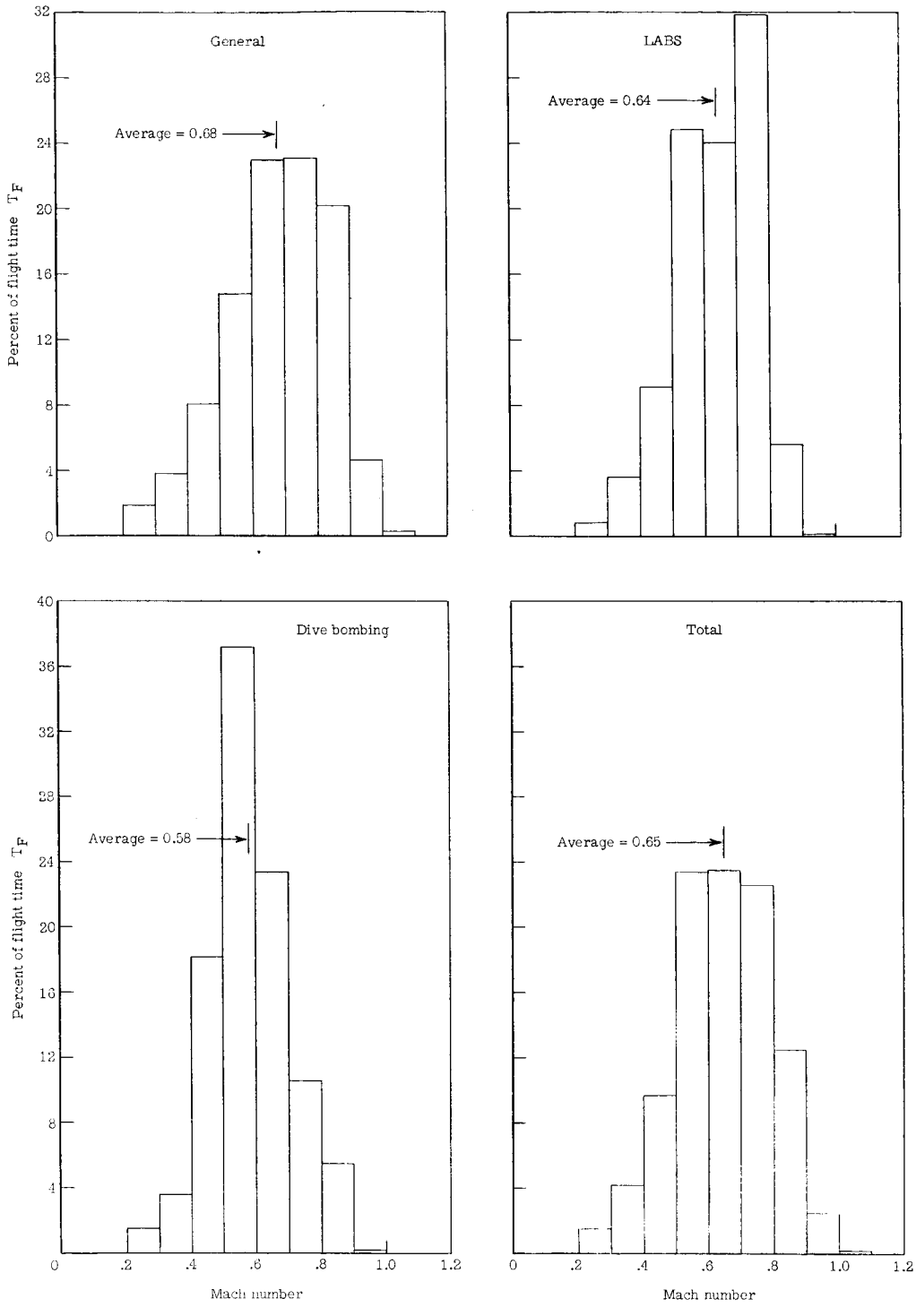

Figure 4.- Distribution of Mach number for various types of missions.

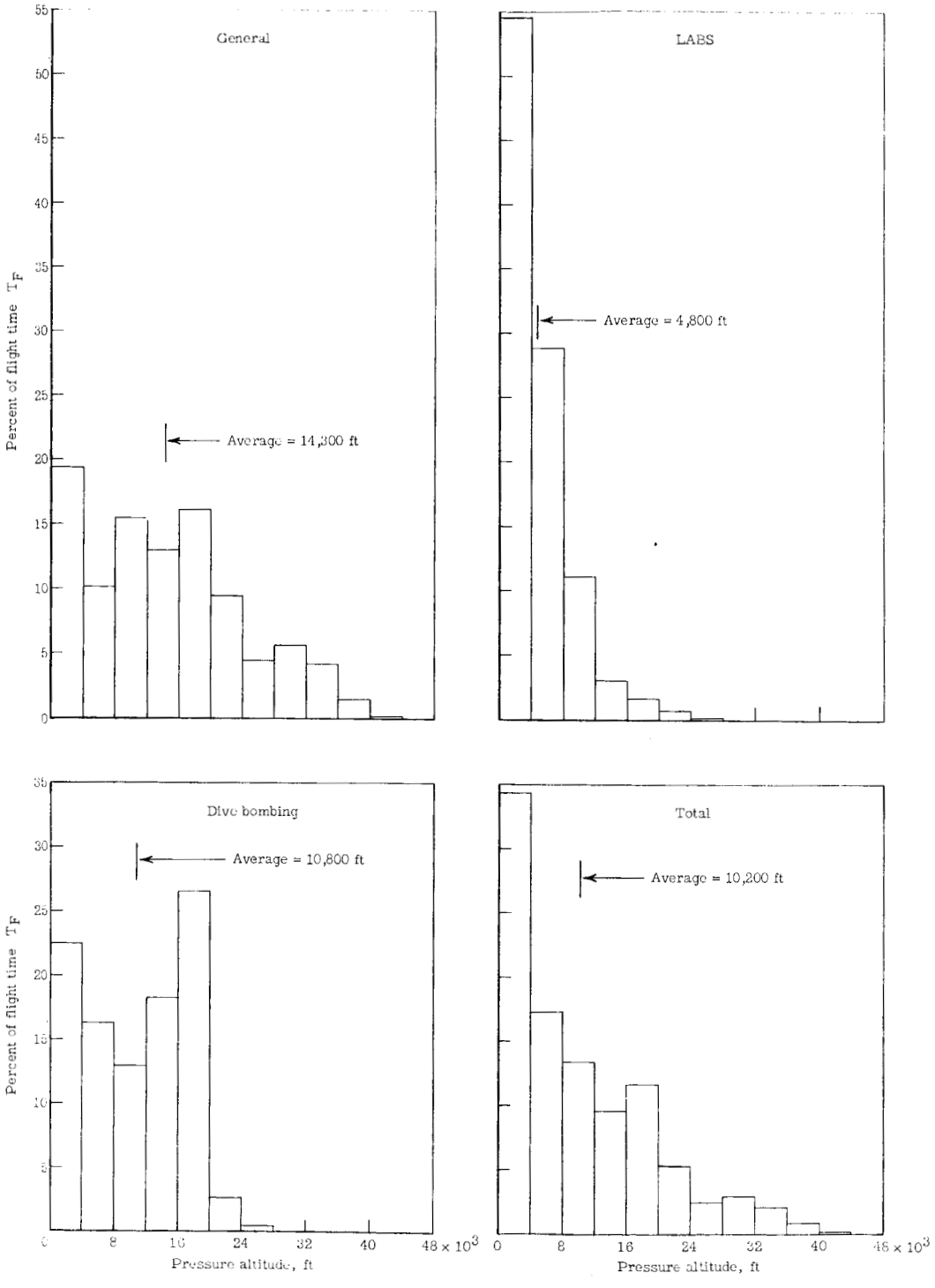

Figure 5.- Distribution of altitude for various types of missions.

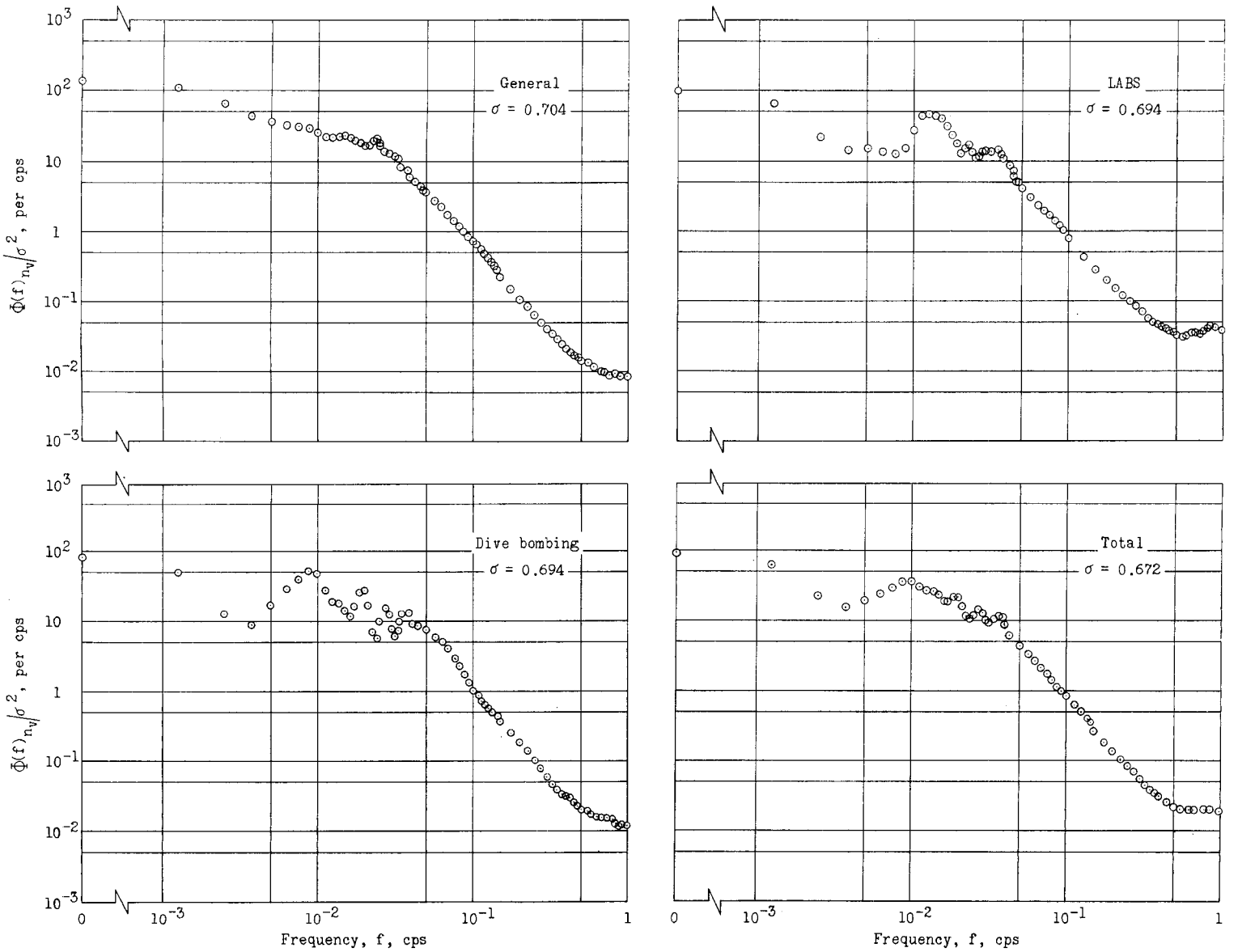

Figure 6.- Power spectral densities of normal load factor for various types of missions.

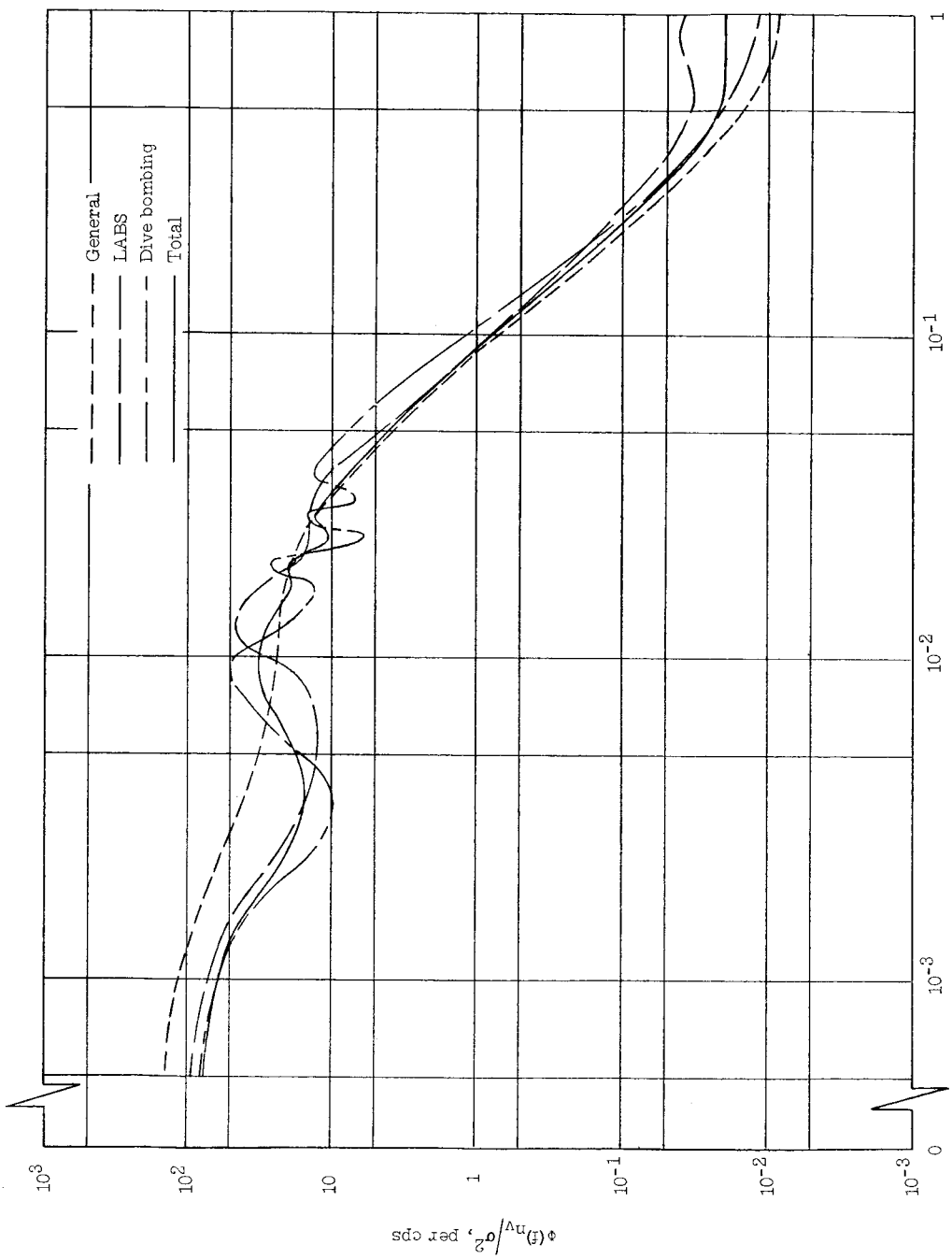

Figure 7.- Comparison of the frequency content for normal load factor during various types of missions.

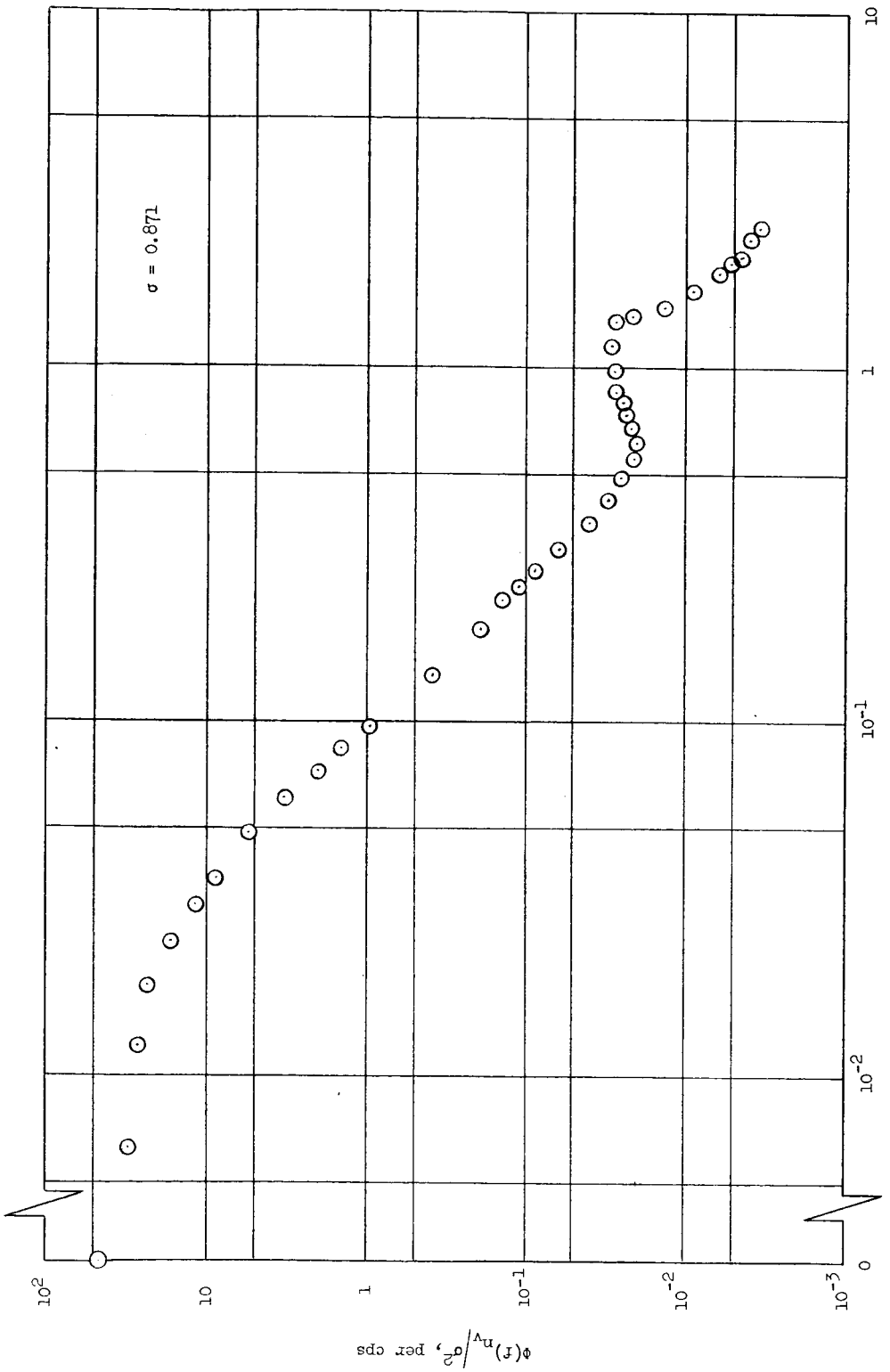

Figure 8.- Power spectral densities of normal load factor for one low-altitude-bombing flight.

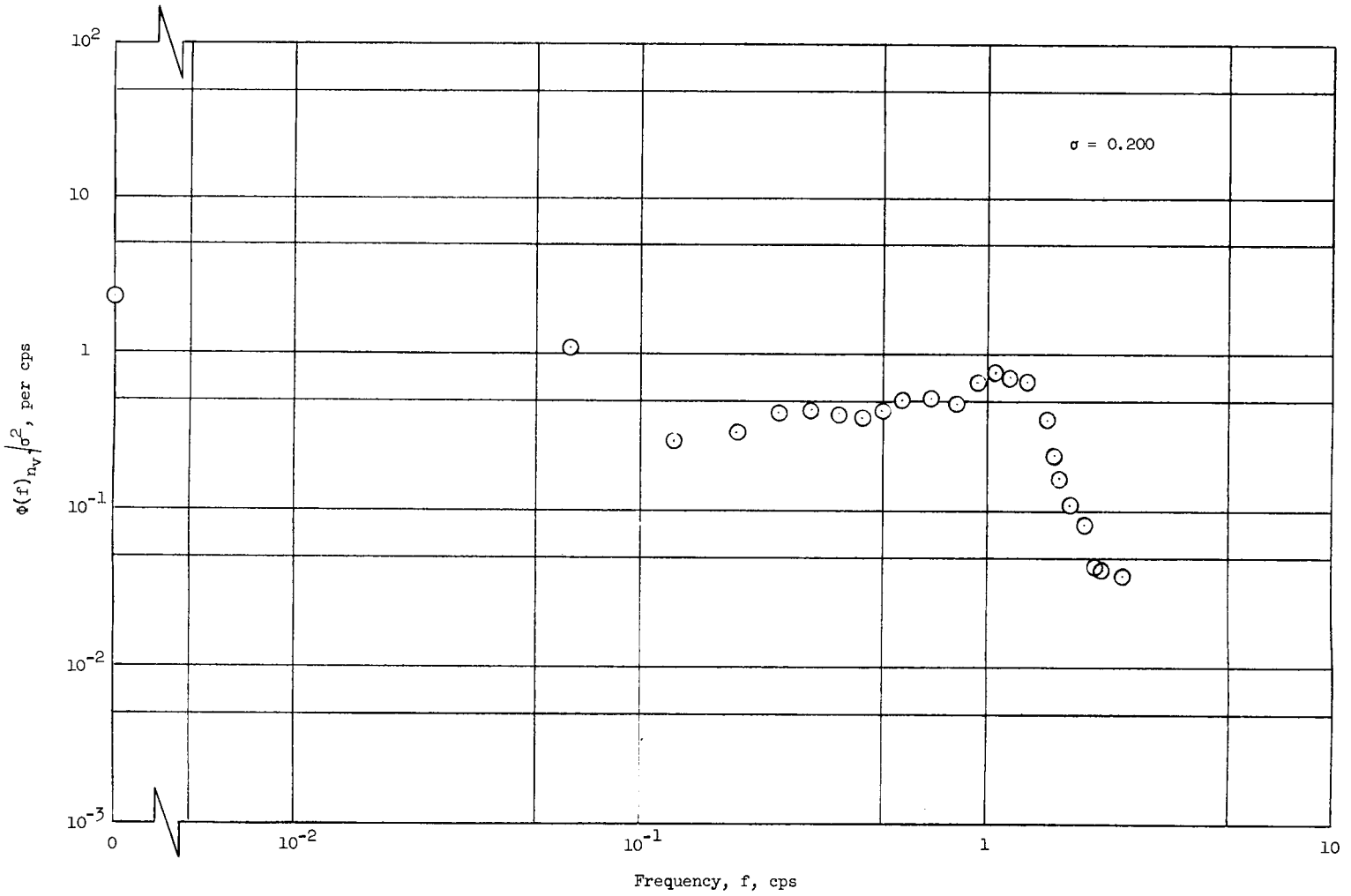

Figure 9.- Power spectral densities of normal load factor for a straight and level flight through rough air.

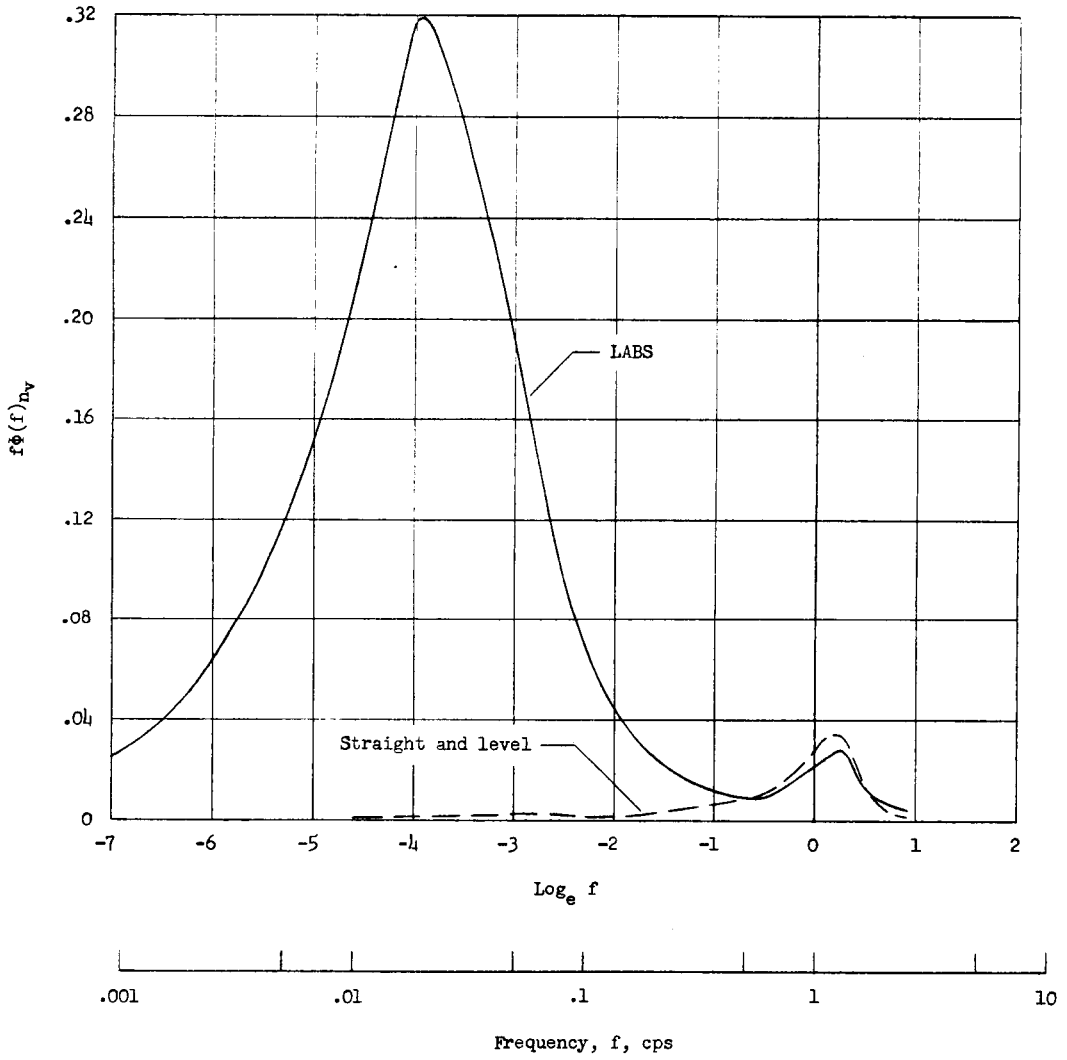

Figure 10.- Illustration of significant frequency range in normal-load-factor spectra for maneuvering and nonmaneuvering flight in rough air.

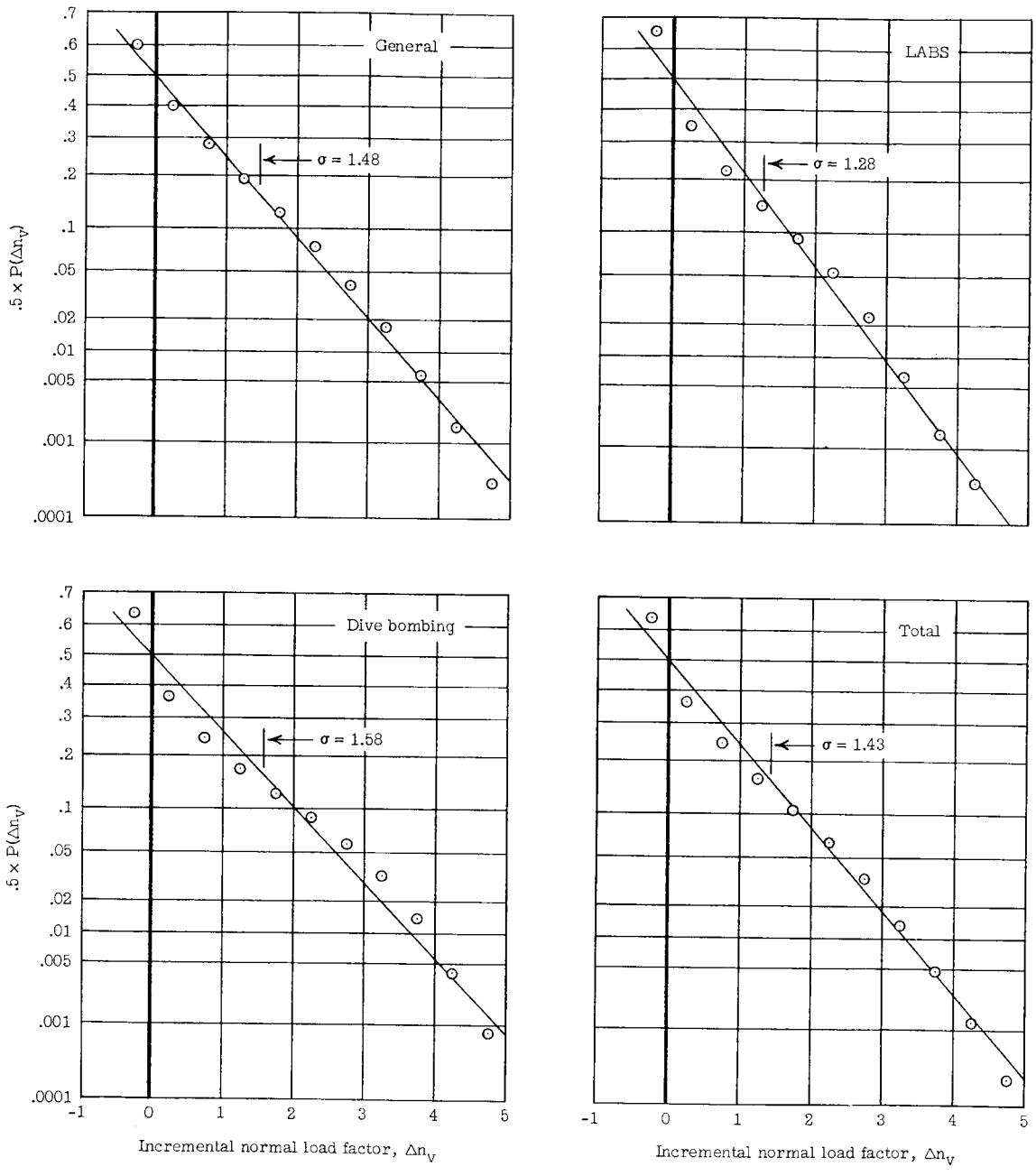

Figure 11.- Comparison of observed probability distributions of incremental-normal-load-factor threshold counts with truncated normal probability distributions for various types of missions.

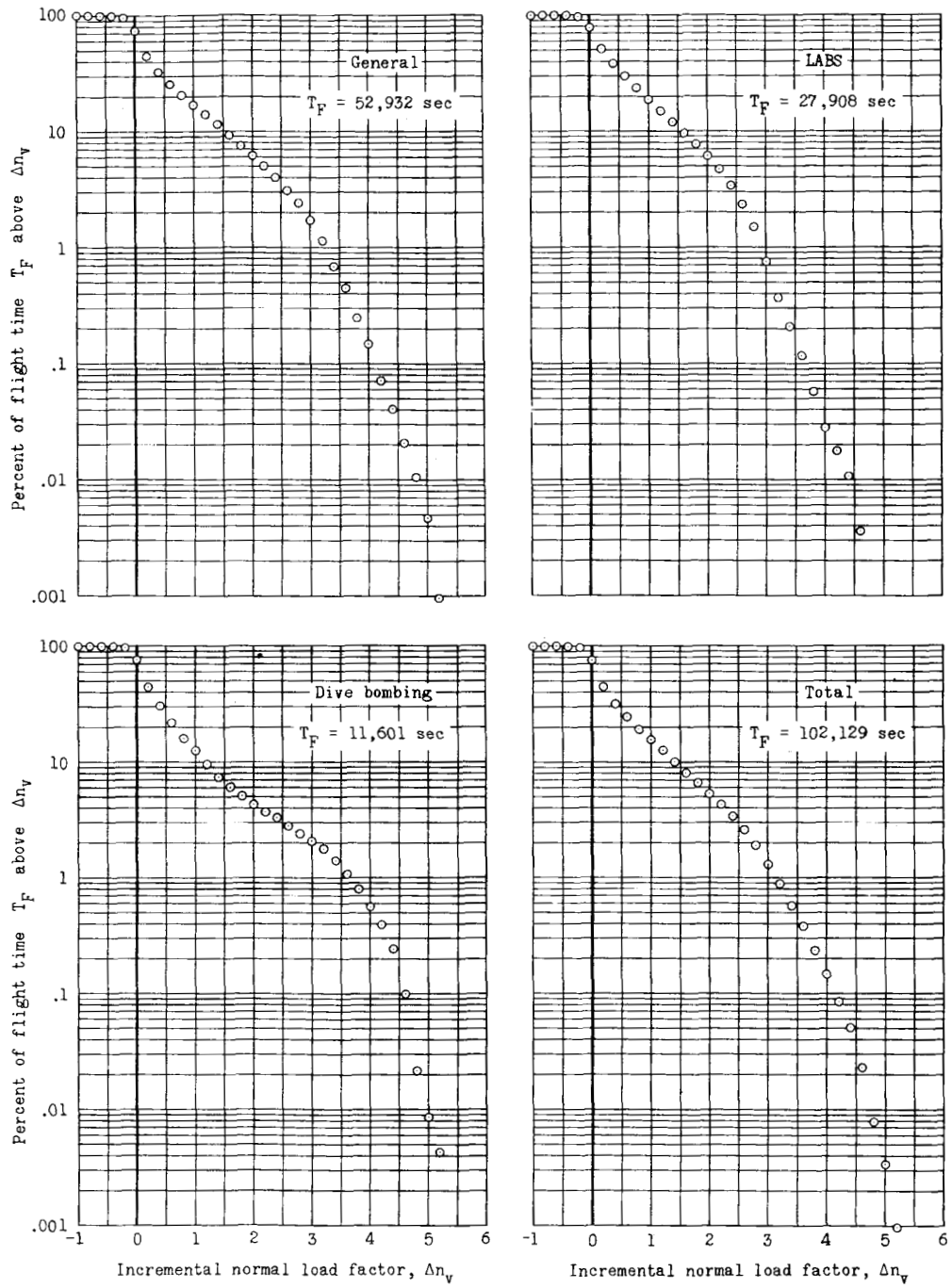

Figure 12.- Percentage of flight time T_F spent above a given incremental normal load factor for various types of missions.

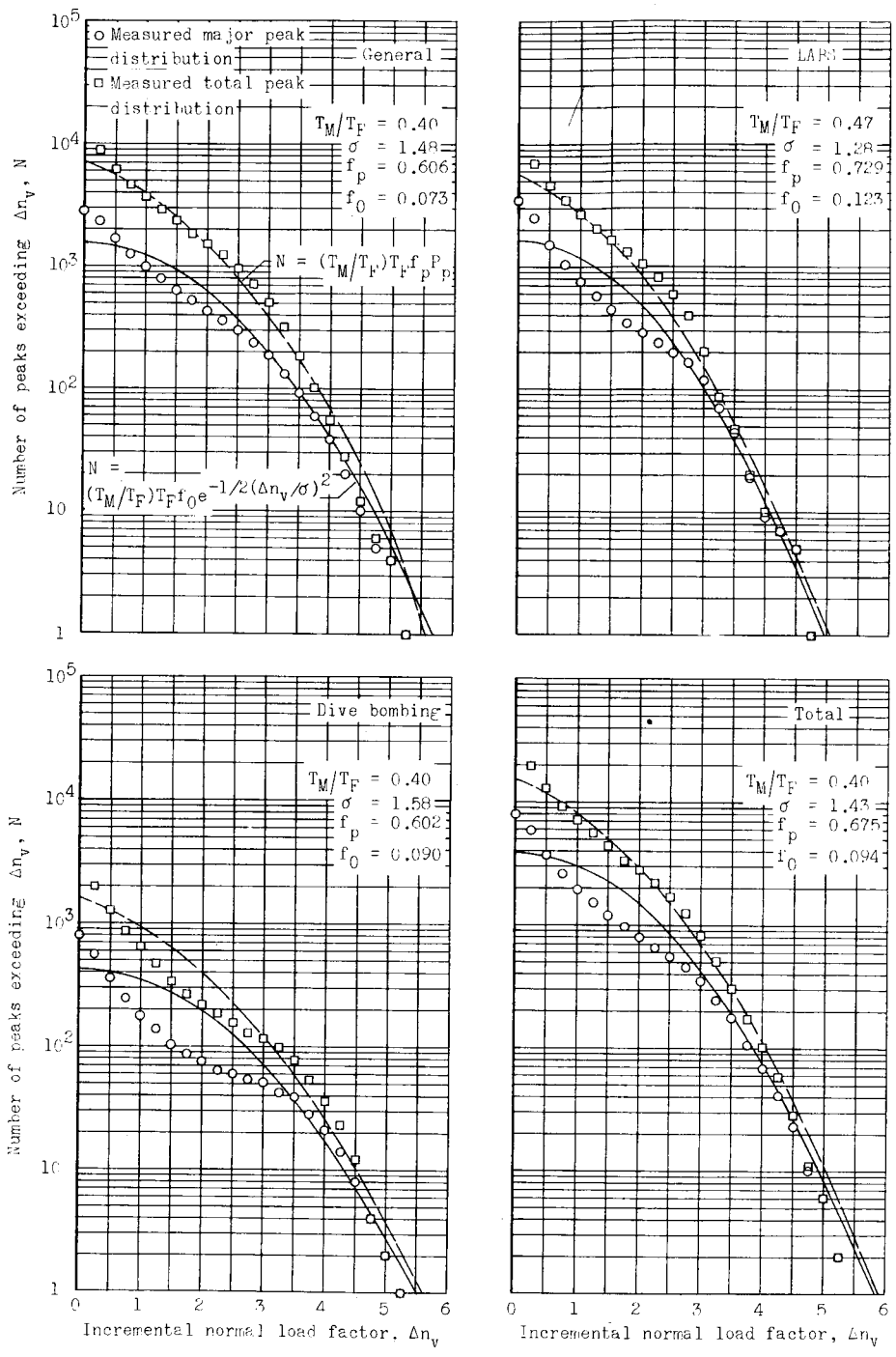

Figure 13.- Comparison of observed incremental normal-load-factor peak distributions with those calculated from power spectra for various types of missions.

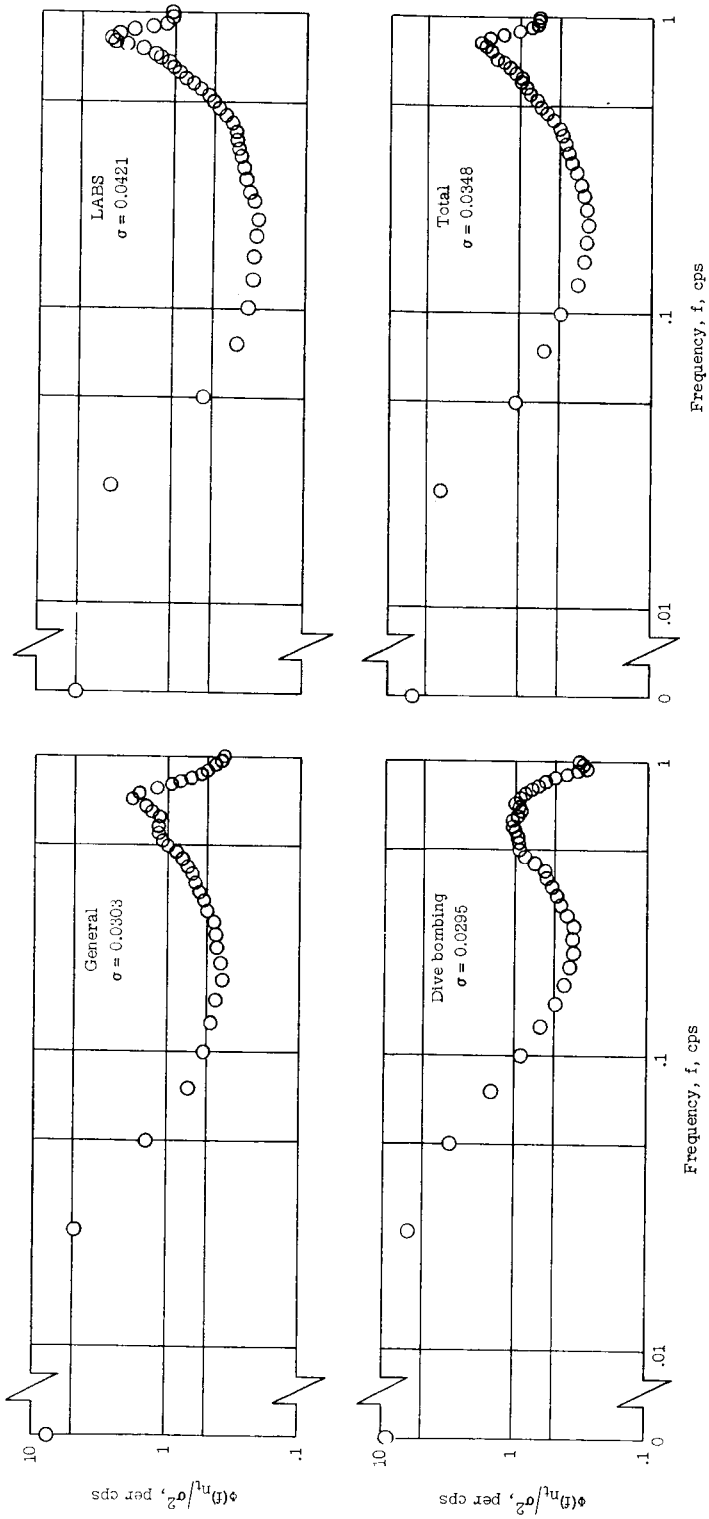

Figure 14.- Power spectral densities of transverse load factor for various types of missions.

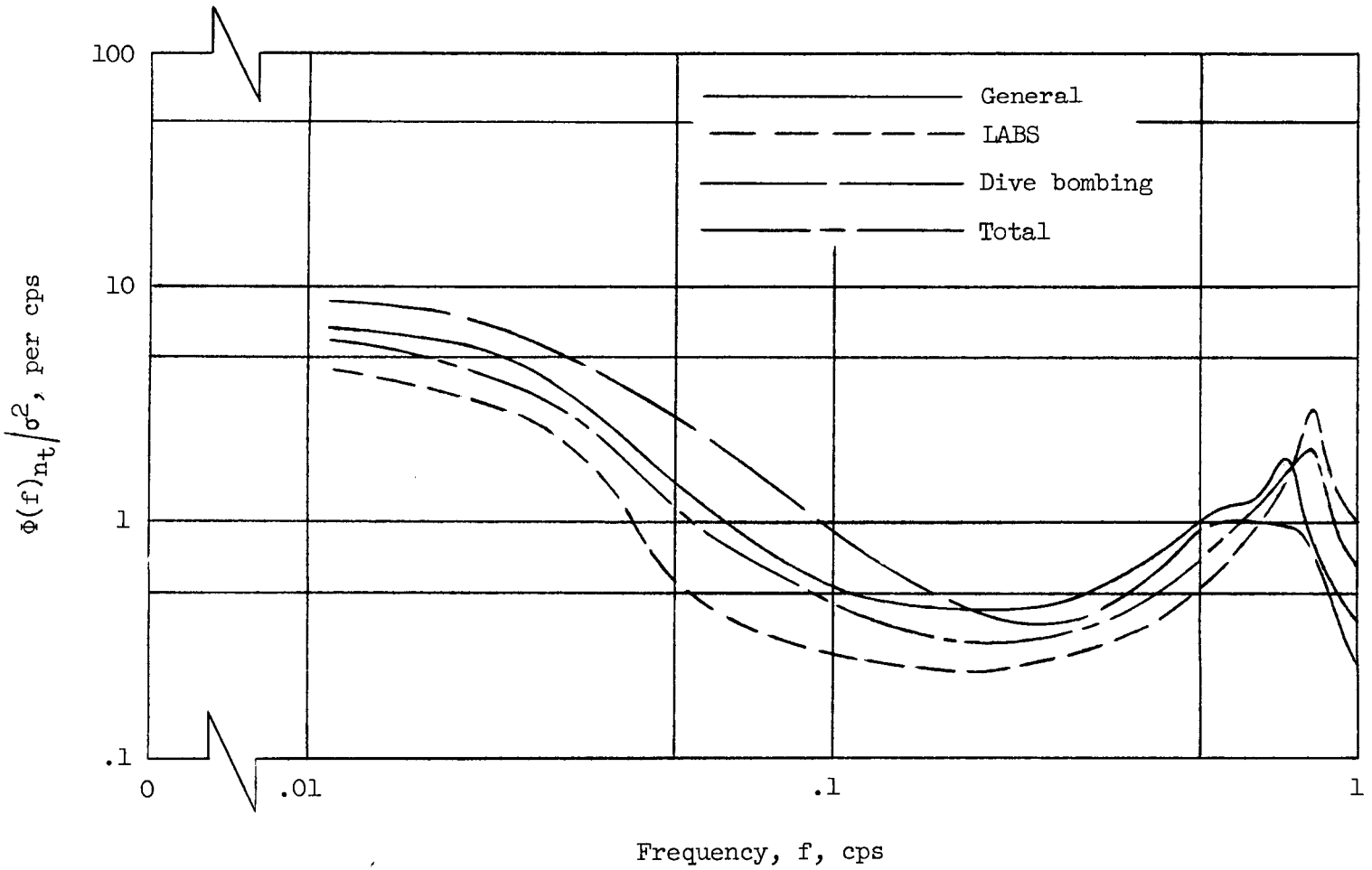

Figure 15.- Comparison of the frequency content for transverse load factor during various types of missions.

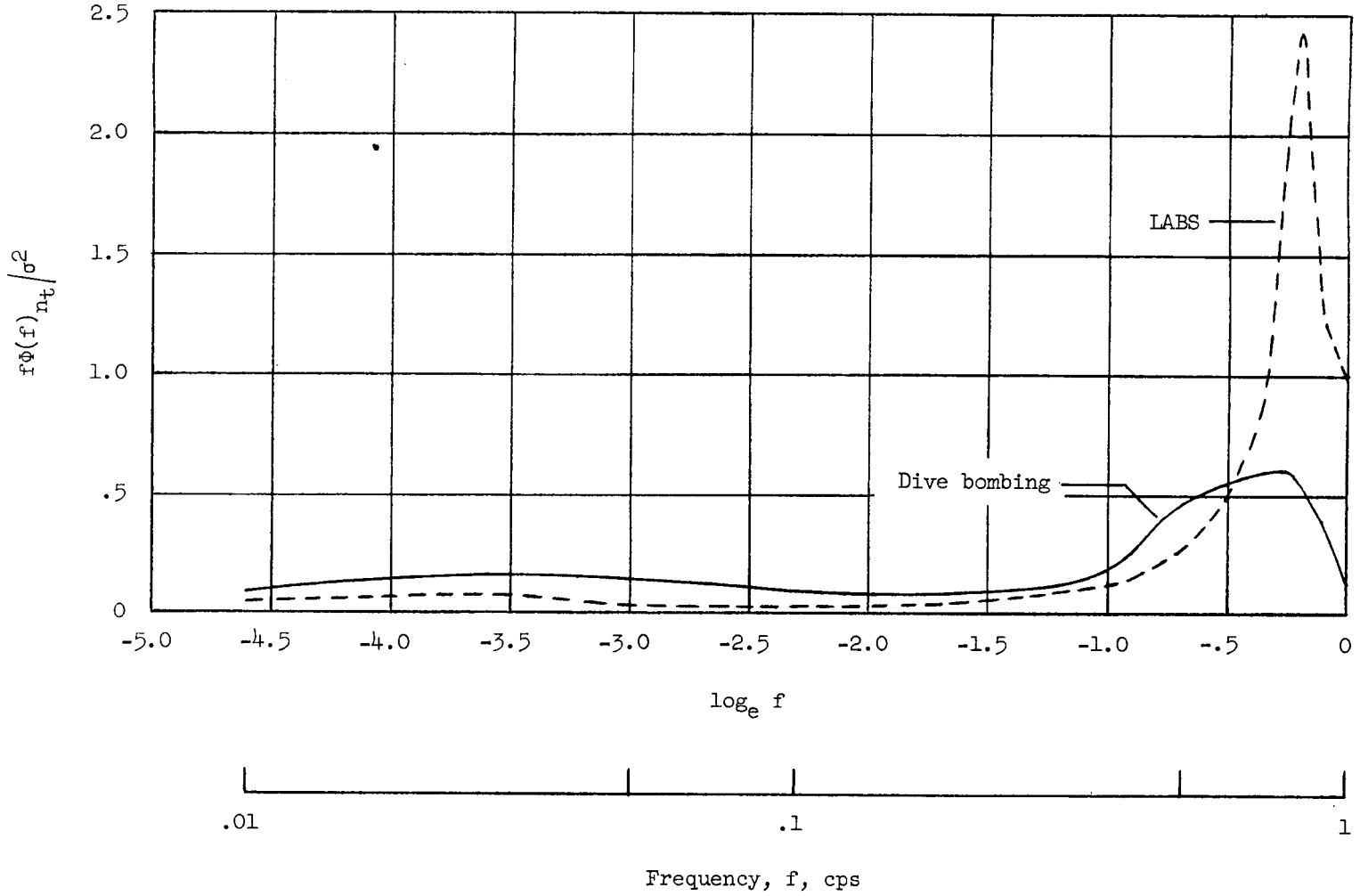

Figure 16.- Illustration of significant frequency range in transverse-load-factor spectra for two types of missions.

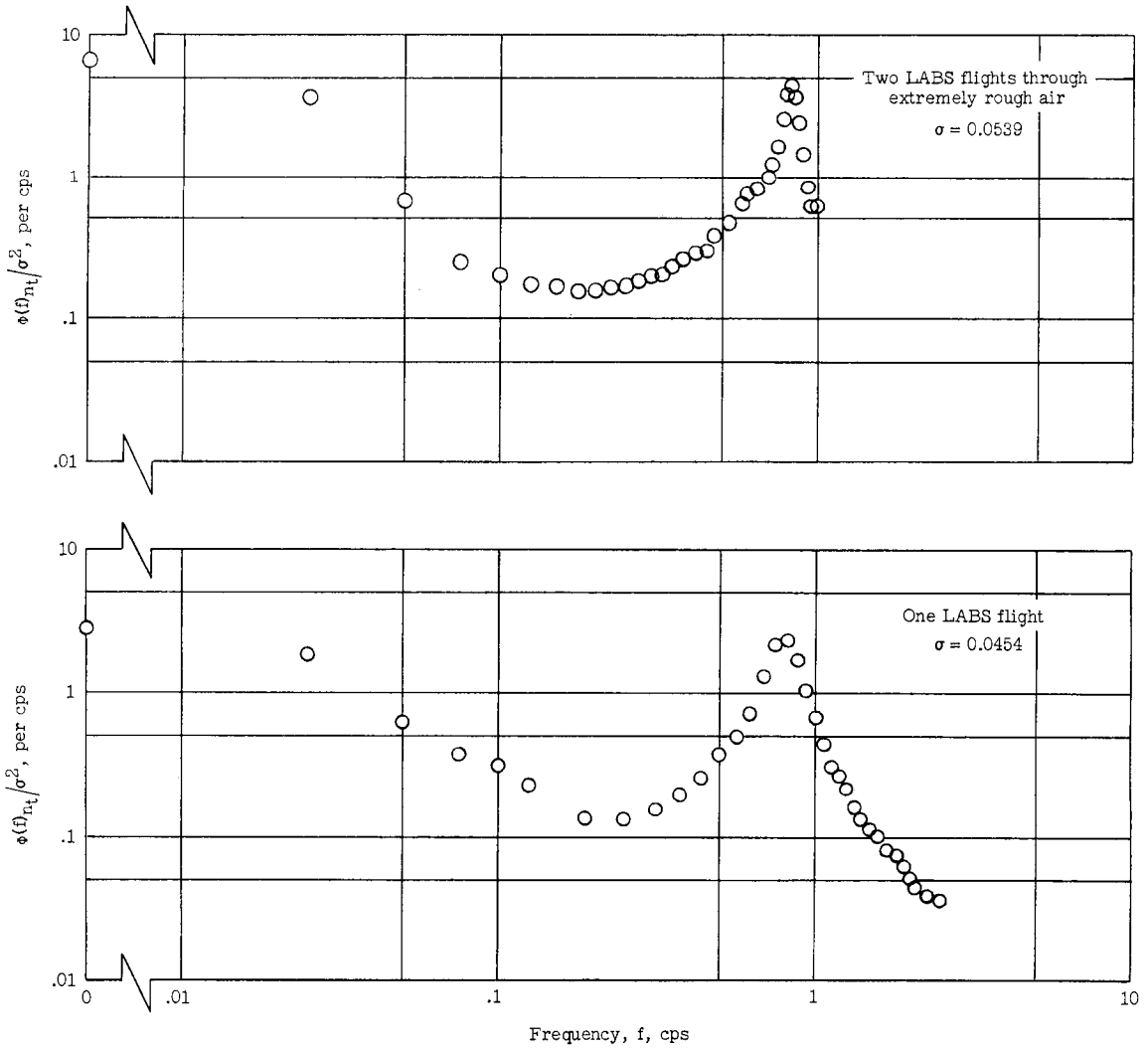

Figure 17.- Power spectral densities of transverse load factor for several low-altitude-bombing flights.

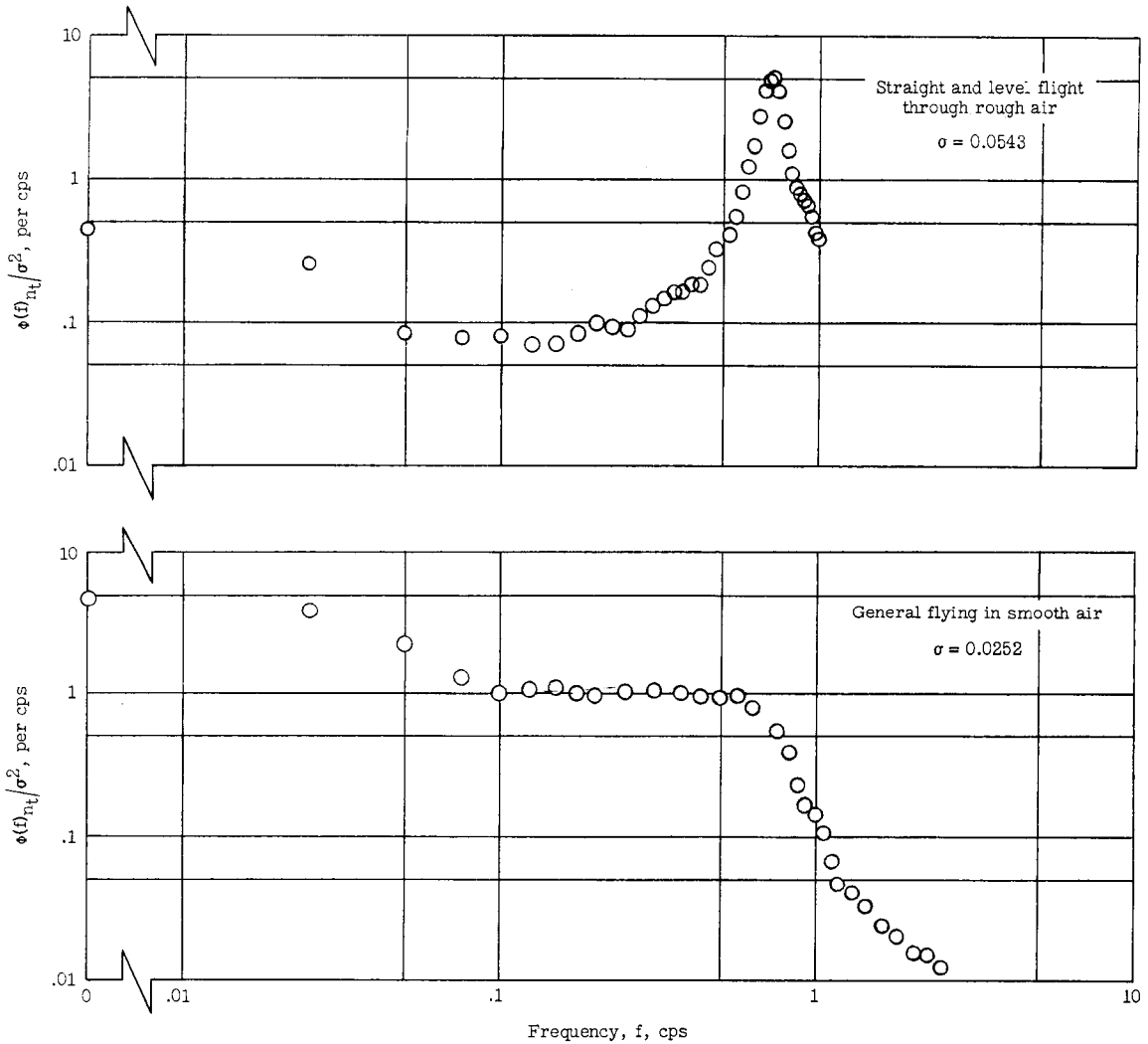

Figure 18.- Power spectral densities of transverse load factor for a straight and level flight through rough air and for a maneuvering flight in smooth air.

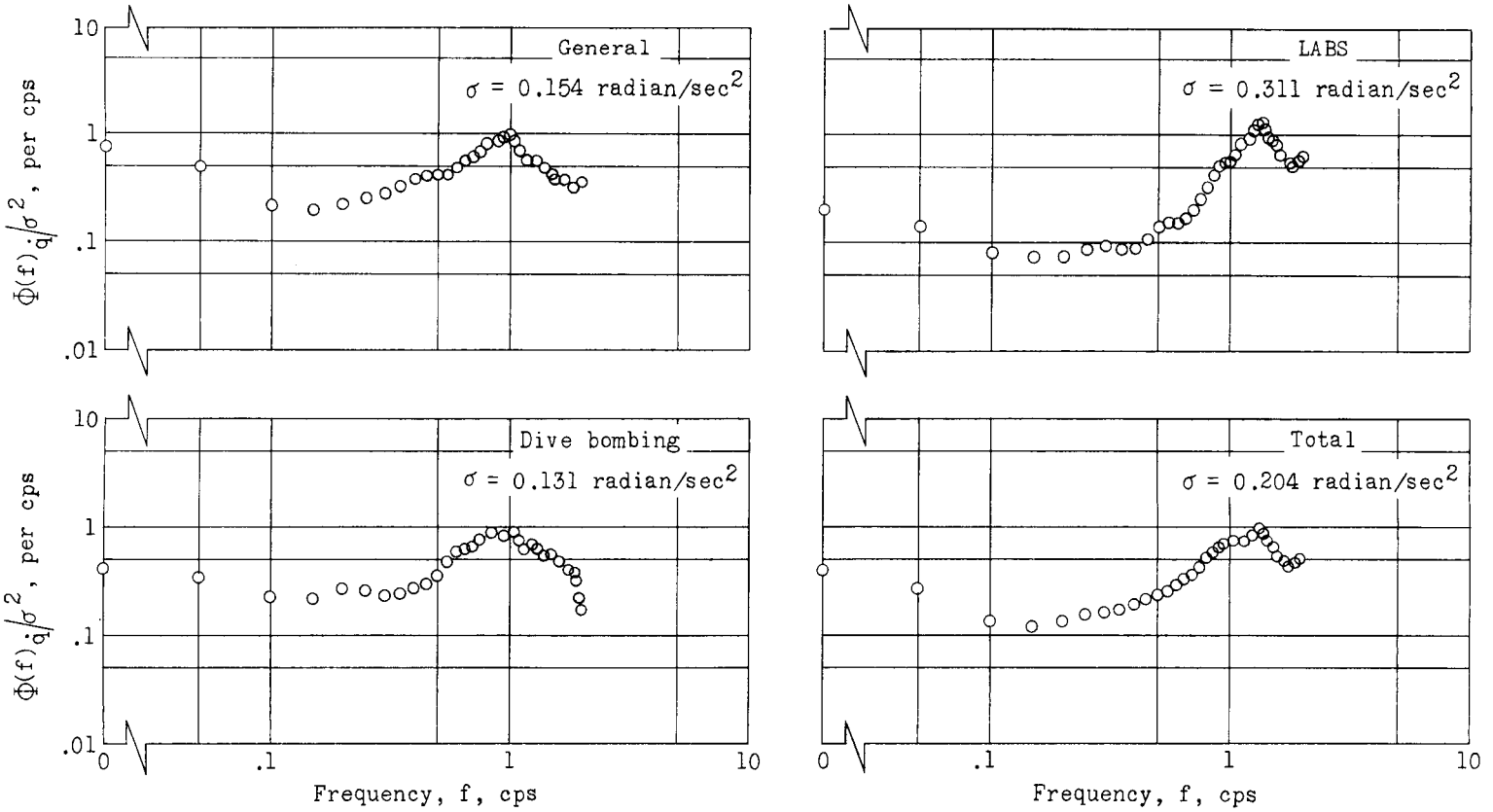

Figure 19.- Power spectral densities of pitching acceleration for various types of missions.

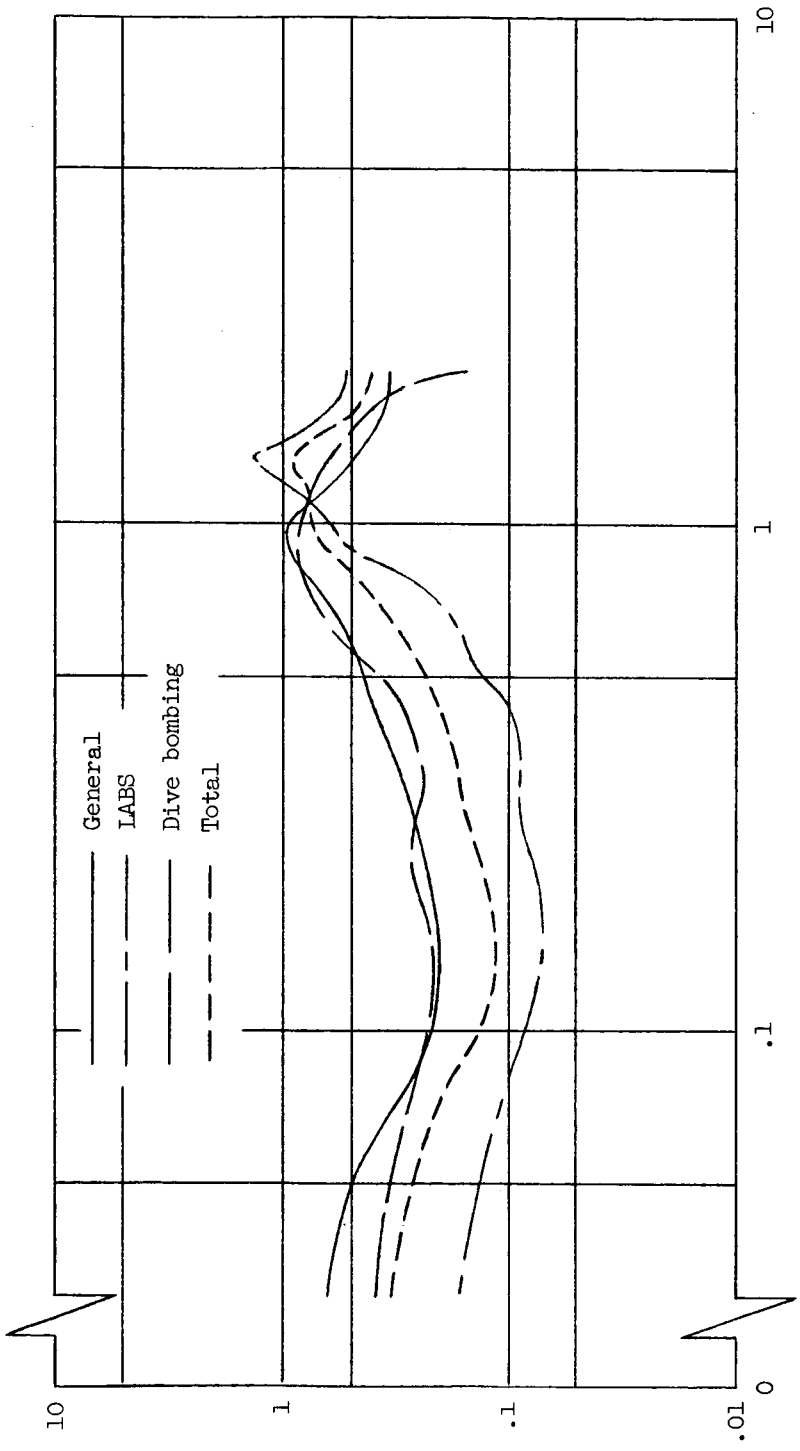

Figure 20.- Comparison of the frequency content for pitching acceleration during various types of missions.